

Yb Integrates piRNA Intermediates and Processing Factors into Perinuclear Bodies to Enhance piRISC Assembly

Yukiko Murota,^{1,2,6} Hirotugu Ishizu,^{3,6} Shinichi Nakagawa,⁴ Yuka W. Iwasaki,² Shinsuke Shibata,⁵ Mihar K. Kamatani,² Kuniaki Saito,² Hideyuki Okano,⁵ Haruhiko Siomi,² and Mikiko C. Siomi^{3,*}

¹Institute for Genome Research, University of Tokushima, Tokushima 770-8503, Japan

²Department of Molecular Biology, Keio University School of Medicine, Tokyo 160-8582, Japan

³Department of Biological Sciences, Graduate School of Science, The University of Tokyo, Tokyo 113-0032, Japan

⁴RIKEN, Wako, Saitama 351-0198, Japan

⁵Department of Biomedical Physiology, Keio University School of Medicine, Tokyo 160-8582, Japan

⁶Co-first author

*Correspondence: siomim@bs.s.u-tokyo.ac.jp

<http://dx.doi.org/10.1016/j.celrep.2014.05.043>

This is an open access article under the CC BY-NC-ND license (<http://creativecommons.org/licenses/by-nc-nd/3.0/>).

SUMMARY

PIWI-interacting RNAs (piRNAs) direct Piwi to repress transposons and maintain genome integrity in *Drosophila* ovarian somatic cells. piRNA maturation and association with Piwi occur at perinuclear Yb bodies, the centers of piRNA biogenesis. Here, we show that piRNA intermediates arising from the piRNA cluster *flamenco* (*flam*) localize to perinuclear foci adjacent to Yb bodies, termed Flam bodies. RNAi-based screening of piRNA factors revealed that Flam body formation depends on Yb, the core component of Yb bodies, while Piwi and another Yb body component, Armitage, are dispensable for formation. Abolishing the RNA-binding activity of Yb disrupts both Flam bodies and Yb bodies. Yb directly binds *flam*, but not transcripts from neighboring protein-coding genes. Thus, Yb integrates piRNA intermediates and piRNA processing factors selectively into Flam bodies and Yb bodies, respectively. We suggest that Yb is a key upstream factor in the cytoplasmic phase of the piRNA pathway in ovarian somatic cells.

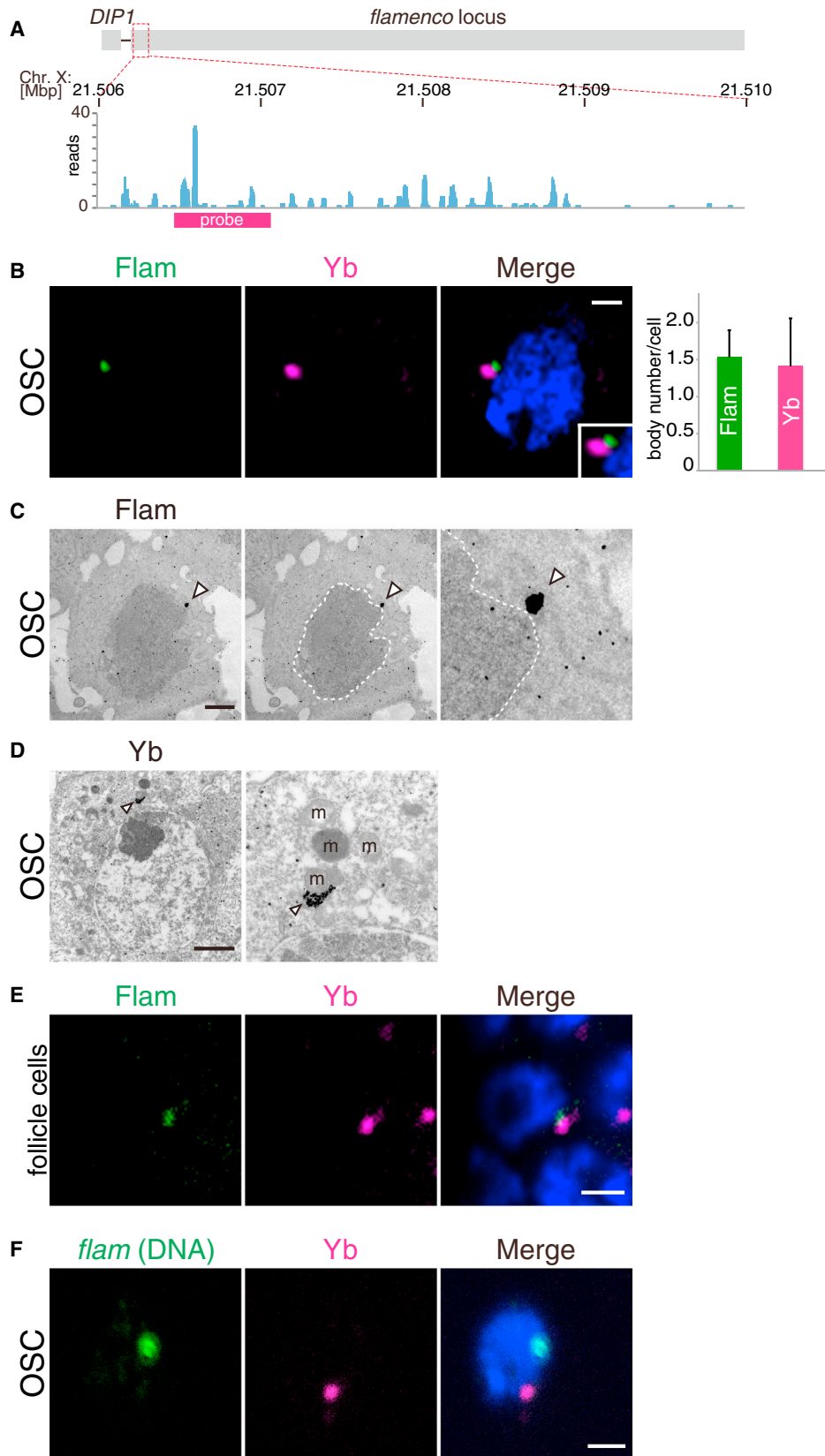
INTRODUCTION

PIWI-interacting RNAs (piRNAs) are small noncoding RNAs of 23–30 nt that are enriched in animal germlines. piRNAs specifically interact with PIWI proteins to form piRNA-induced silencing complexes (piRISCs) and direct them to repress transposons and thus maintain genome integrity in the gonads (Ishizu et al., 2012; Juliano et al., 2011; Siomi et al., 2011). Loss-of-function mutations of PIWI proteins or piRNA biogenesis impairment cause derepression of transposons, leading to defects in gametogenesis and sterility (Aravin et al., 2007; Khurana and Theurkauf, 2010).

Drosophila express three PIWI proteins: Piwi, Aubergine (Aub), and AGO3 (Siomi et al., 2011). In germ cells in the ovaries, primary piRNAs originate from intergenic piRNA clusters through the primary piRNA processing pathway in a Dicer-independent fashion and are loaded onto Piwi and Aub. Following this, Piwi localizes to the nucleus to mediate transposon silencing. In contrast, Aub localizes to the cytoplasm, where it plays a role in the piRNA amplification cycle cooperating with AGO3 through reciprocal RNA cleavage that depends on PIWI-Slicer (endonuclease) activity (Brennecke et al., 2007; Gunawardane et al., 2007; Ishizu et al., 2012; Malone et al., 2009). In this system, transposon transcripts in both sense and antisense orientations are consumed as piRNA precursors; thus, transposon silencing and piRNA production occur simultaneously, enabling a constant supply of piRNAs in cells.

Somatic cells in ovaries express Piwi, but not Aub or AGO3; therefore, they fail to amplify piRNAs. Thus, all piRNAs are primary and are specifically loaded onto Piwi (Ishizu et al., 2012). The Piwi-piRNA complex is then translocated to the nucleus, in which it implements transcriptional silencing in cooperation with cofactors such as Maelstrom and DmGTSF1/Asterix (Döntert et al., 2013; Muerdter et al., 2013; Ohtani et al., 2013; Sienski et al., 2012). Whether Piwi in germ cells analogously collaborates with Maelstrom and DmGTSF1/Asterix to achieve transposon repression remains unknown.

Investigation of the primary piRNA pathway using a cultured *Drosophila* ovarian somatic cell (OSC) line and fly ovaries has revealed that perinuclear Yb bodies are the centers for piRNA processing and piRISC formation in ovarian somatic cells (Olivieri et al., 2010; Saito et al., 2010). Protein constituents of Yb bodies include Yb, Armitage (Armi), Shutdown (Shu), Sister of Yb (SoYb) and Vreteno (Vret), all of which contain domains associated with RNA metabolism; for instance, Yb shows significant similarity to DEAD-box proteins and contains a Tudor (Tud) domain, whereas Vret contains two Tud domains and an RNA-recognition motif (Ishizu et al., 2012). Armi belongs to the Upf1p family of ATP-dependent RNA helicase (Cook et al., 2004). Loss of Yb body components prevents accumulation of primary piRNAs in the



(legend on next page)

soma; thus, they are all required for primary piRNA biogenesis and gonadal development (Haase et al., 2010; Handler et al., 2011; Olivieri et al., 2010, 2012; Qi et al., 2011; Saito et al., 2010; Szakmary et al., 2009; Zamparini et al., 2011).

Nascent, piRNA-unloaded Piwi in OSCs interacts with Armi and Yb, and the resultant complex associates with piRNA intermediates in Yb bodies (Olivieri et al., 2010; Saito et al., 2010). Depletion of Yb disrupts Yb bodies, liberating other components into the cytosol. Under these conditions, Piwi and Armi still associate, although the heterodimer does not contain piRNA intermediates. As a result, piRISC formation fails. It is likely that Yb is at the top of the hierarchy for Yb body formation and piRISC formation and that Armi, although categorized as an RNA helicase based on peptide sequence similarity, binds RNA substrates (piRNA intermediates) upon localization to Yb bodies.

Zucchini (Zuc), a phospholipase D superfamily member, is a single-strand-specific endonuclease required for converting piRNA intermediates to mature piRNAs (Ipsaro et al., 2012; Nishimasu et al., 2012). Depletion of Zuc in OSCs results in dispersal of Yb bodies, because piRNA-unloaded Piwi is stalled and fails to localize to the nucleus (Saito et al., 2010). Without Zuc, an excess of unprocessed piRNA intermediates accumulate in OSCs as ribonucleoprotein (RNP) complexes with Armi, Yb, and Piwi; as a result, few piRNAs are produced (Haase et al., 2010; Nishimasu et al., 2012; Saito et al., 2010). These defects can be rescued by ectopic expression of wild-type (WT) Zuc, but not by ectopic expression of endonuclease-deficient Zuc mutants (Nishimasu et al., 2012). Zuc has a mitochondrial targeting signal at the N terminus, and indeed mouse Zuc (also known as MitoPLD) localizes to the outer membranes of mitochondria, facing into the cytosol in mammalian cells (Choi et al., 2006). Zuc signals in OSCs can be detected in close proximity to Yb bodies (Saito et al., 2010), as pi-bodies and piP-bodies, which are considered to be the sites of piRNA biogenesis in mouse testis, are located in intermitochondrial regions (Pillai and Chuma, 2012). This type of intracellular architectural arrangement might raise the rates of Zuc-mediated conversion of piRNA intermediates to mature piRNAs in the cells.

The functions of piRNA protein factors have been well studied. In contrast, the cell biology of piRNA precursors is poorly understood. Therefore, in this study, we performed RNA-fluorescence in situ hybridization (RNA-FISH) in OSCs to visualize RNA transcripts arising from the *flamenco* (*flam*) piRNA cluster. *flam* is the main source of primary piRNAs in OSCs and somatic follicle cells in *Drosophila* ovaries (Brennecke et al., 2007; Malone et al.,

2009; Saito et al., 2009). A P-element insertion in *flam* causes derepression of transposons such as *gypsy* and piRNA loss in mutant follicle cells (Brennecke et al., 2007; Mével-Ninio et al., 2007). RNA-FISH showed that *flam* transcripts are condensed into perinuclear foci adjacent to Yb bodies, which we termed Flam bodies. Recently, a similar type of body named “Dot COM” was reported (Dennis et al., 2013). The similarities and differences between Flam bodies and Dot COM will be described below. RNAi-based screening of piRNA factors revealed that Flam body formation depends on Yb, the core component of Yb bodies, while Piwi and another Yb body component, Armi, are dispensable for the assembly. Depletion of Zuc, which causes excessive accumulation of unprocessed piRNA intermediates (Haase et al., 2010; Nishimasu et al., 2012), results in the dispersion of Flam bodies, which overlap considerably with Yb bodies. Abolishing the RNA-binding activity of Yb disrupts both Flam bodies and Yb bodies. Yb directly binds *flam* transcripts, but not the transcripts of a neighboring protein-coding gene, *DIP1*. Thus, Yb integrates piRNA intermediates and piRNA processing factors selectively into Flam bodies and Yb bodies, respectively. We propose that Yb is a key upstream factor in the cytoplasmic phase of the piRNA pathway in the ovarian soma.

RESULTS

flam Transcripts Are Localized to Perinuclear Flam Bodies in Ovarian Soma

To examine the cellular localization of *flam* transcripts in OSCs, we performed RNA-FISH using a *flam*-specific riboprobe complementary to the 5' region of the *flam* transcript (Figure 1A). This region produces a substantial amount of primary piRNAs in OSCs (Saito et al., 2010) (Figure 1A). By RNA-FISH, perinuclear, punctate signals were observed, suggesting that the *flam*-piRNA precursors/intermediates concentrate at the cytoplasmic bodies (Figures 1B and S1A). A recent report showed that *flam*/COM transcripts (*flam* is also known as COM) are enriched in a single nuclear focus, termed Dot COM (Dennis et al., 2013). However, using electron microscopy in situ hybridization (EM-ISH), we detected *flam* signals in the cytoplasm (Figures 1C and S1B). Fluorescence quantification analysis revealed that the average number of Flam bodies per cell was 1.5 (Figure 1B). Signals from RNA-FISH riboprobes that were used originally by Dennis et al. (COM 508 and 527) (Dennis et al., 2013) coincided with the *flam* signals (Figure S1C). Hereinafter,

Figure 1. Flam Bodies Localize Adjacent to Yb Bodies in *Drosophila* Ovarian Soma

(A) Schematic drawing of the genomic *flam* locus and an upstream protein-coding gene *DIP1* on chromosome X. Mature piRNAs uniquely mapping to the 5' region of the *flam* locus corresponding to 21,506,000 to 21,510,000 on chromosome X (Saito et al., 2009) are shown by blue bars. A 583 nt riboprobe for RNA-FISH complementary to the *flam* transcripts is shown by a magenta box (probe) (chrX: 21,506,472–21,507,054).

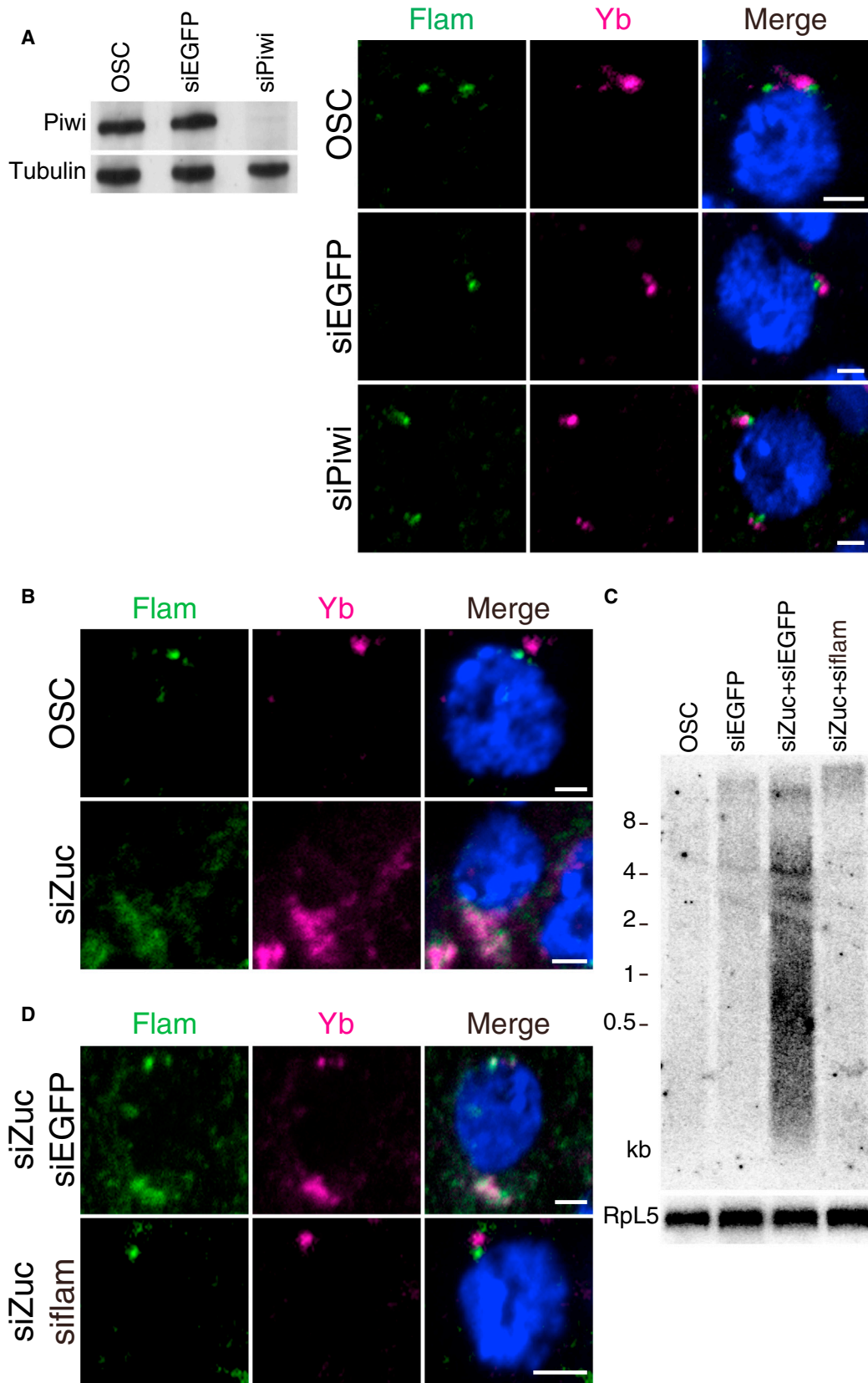
(B) Flam body (green) and Yb body (magenta) in OSCs visualized by RNA-FISH and immunofluorescence using anti-Yb antibody, respectively. The nucleus is stained with DAPI (blue). Scale bar, 2 μ m. The numbers of Flam bodies and Yb bodies were determined by quantification analysis of *flam* and Yb signals in OSCs (n = 20).

(C) Electron microscope in situ hybridization using the probe shown in (A) detects a *flam* signal (white arrowhead) in the cytoplasm of OSC. The far-right image is an enlarged image of the middle image (partial). A white dot line shows where the nucleus is. Scale bar, 2 μ m.

(D) Immunoelectron microscopy using anti-Yb antibody shows a perinuclear Yb body in an OSC (white arrowhead). The right-hand image is an enlarged image of the left-side image (partial). m, mitochondria. Scale bar, 2 μ m.

(E) Flam body (green) and Yb bodies (magenta) in follicular cells of *Drosophila* ovaries. The nuclei are stained with DAPI (blue). Scale bar, 2 μ m.

(F) The *flam* loci (green) in the nucleus and Yb body (magenta) in the cytoplasm. The nucleus is stained with DAPI (blue). Scale bar, 2 μ m.



(legend on next page)

we refer to the *flam*-positive, perinuclear bodies as Flam bodies.

Flam bodies appear to be similar to Yb bodies, both in size and number. Therefore, we set out to understand the spatial relationship between Flam bodies and Yb bodies in OSCs by combining *flam* RNA-FISH and immunofluorescence using an anti-Yb antibody that we raised in this study (Figure S1D). Immunoelectron microscopy using the antibody confirmed the perinuclear localization of Yb bodies (Figure 1D). Flam bodies were frequently located adjacent to Yb bodies and tended to be closer to the nucleus than Yb bodies (Figures 1B and S1A). The average number of Yb bodies was similar to that of Flam bodies (1.4 per cell) (Figure 1B). Both signals were also detected in the somatic follicle cells of *Drosophila* ovaries (Figures 1E and S1E). Thus, they are not specific for cultured cells. In *flam* mutant follicle cells, Flam bodies were not detected, confirming the specificity of the RNA-FISH probe (Figure S1F). EM-ISH confirmed the cytoplasmic localization of Flam bodies in follicle cells (Figure S1G). DNA-FISH (Figure S1H) was conducted concomitantly with immunofluorescence using the anti-Yb antibody. No spatial correlation was found between *flam* nuclear foci and Yb bodies (Figures 1F and S1I).

Flam Bodies Are Not the Sites of Mature piRNA Accumulation

It is possible that mature *flam*-piRNAs, rather than their intermediates and/or full transcripts, might be the major components of Flam bodies. To examine this, we visualized Flam bodies and Yb bodies in Piwi-depleted OSCs. Loss of Piwi decreased the level of mature piRNAs drastically (Saito et al., 2009, 2010). This was because Piwi is the sole protein loaded with mature piRNAs in OSCs and, thus, piRNAs are destabilized without Piwi. If mature piRNAs were the major RNA components of Flam bodies, Piwi depletion would cause disappearance of these bodies. However, they were unaffected by Piwi depletion (Figure 2A). These results indicate that Piwi is dispensable for Flam body formation and that Flam bodies are not the sites of mature piRNA storage.

piRNA Intermediates Concentrate in Flam Bodies

Depletion of Zuc caused Yb body dispersion and stalling of Piwi at Yb bodies (Saito et al., 2010). This particular fraction of Piwi was associated with few or no mature piRNAs, although the Armi complex containing Yb and Piwi still bound piRNA intermediates (Saito et al., 2010). These phenomena correlate well with our recent finding that Zuc is the endoribonuclease necessary for converting piRNA intermediates to mature piRNAs (i.e., piRNA maturation) (Nishimasu et al., 2012). We asked if Flam body for-

mation is affected by loss of Zuc. RNA-FISH in Zuc-depleted OSCs showed that Flam bodies were dispersed similarly to Yb bodies (Figure 2B). Interestingly, the two fluorescent signals were superimposed (Figure 2B). We speculated that the increased level of piRNA intermediates might have caused the superimposition. To examine this, northern blotting was performed to detect *flam* transcripts using probes designed to recognize the 5' end region of *flam* (the "probe" region in Figure 1A). In naive OSCs, a smeary signal for *flam* transcripts was only slightly detected, although Flam bodies were clearly visible by RNA-FISH (Figures 2B and 2C). However, partial *flam* transcripts, being several hundred to 4,000 nt in length, were aberrantly accumulated upon Zuc depletion (Figures 2C and S2A) in agreement with our earlier observation (Nishimasu et al., 2012). The corresponding signal decreased after treatment of the cells with *flam* small interfering RNAs (siRNAs) targeting the probed *flam* region (Figures 2C and S2A). These results suggest that the smeared northern blot signal mostly reflects *flam*-piRNA intermediates. After transfection of cells with *flam* siRNAs, the fuzzy fluorescent signals of Yb bodies and Flam bodies returned to normal, as in naive OSCs (Figure 2D). We suggest that Flam bodies are where *flam*-piRNA intermediates concentrate and that piRNA intermediates originating from loci other than *flam* would be minor. Treatment of normal OSCs with *flam* siRNAs did not disrupt Flam bodies (Figure S2B) and barely affected the levels of *flam* transcripts (Figure S2C), although *flam* siRNAs effectively downregulated *flam* transcripts in Zuc-depleted cells (Figure 2C). *flam* siRNAs were designed to target the region corresponding to the *flam* RNA-FISH probe (Figure 1A). Thus, it is plausible that *flam*-piRNA intermediates at Flam bodies would not be accessible to the RNAi machinery under normal conditions likely due to the compactness of the bodies.

Yb Is Necessary for Formation of Both Yb Bodies and Flam Bodies

Depletion of Yb, but not other Yb body components, disrupts Yb body formation (Handler et al., 2011; Saito et al., 2010). We examined if depletion of Yb would affect Flam body formation. Interestingly, neither Flam bodies nor Yb bodies were detected in the cells (Figures 3A and S3A). Expression of siRNA-resistant Yb (Yb WT-r) restored the formation of both structures (Figures 3A and S3A). Thus, Flam bodies depend on Yb for their formation as do Yb bodies. Yb mutant follicle cells contain neither Flam bodies nor Yb bodies (Figure S3B). Depletion of Armi and Vret, other components of Yb bodies (Olivieri et al., 2010), affected neither Flam nor Yb body formation (Figure S3C and data not

Figure 2. Depletion of Zuc, but Not of Piwi, Affects Yb Body and Flam Body Formation

(A) Western blotting shows the efficiency of Piwi depletion. Piwi siRNA (siPiwi) has little effect on Flam body (green) and Yb body (magenta) formation. Enhanced GFP siRNA (siEGFP) was used as a negative control. Nuclei are stained with DAPI (blue). Scale bar, 2 μ m.

(B) Transfection of OSCs with Zuc siRNA (siZuc) led to superimposition of Flam bodies (green) with Yb bodies (magenta). Nuclei are stained with DAPI (blue). Scale bar, 2 μ m.

(C) Northern blotting shows that transfection of OSCs with Zuc siRNA (siZuc) induces aberrant accumulation of *flam*-piRNA intermediates in OSCs. Transfection of Zuc-depleted OSCs with *flam* siRNAs (siflam) targeting the probed *flam* region downregulates the expression of *flam*-piRNA intermediates. Enhanced GFP siRNA (siEGFP) was used as a negative control. *RpL5* mRNA was visualized as a loading control.

(D) Flam bodies (green) and Yb bodies (magenta) in Zuc-depleted OSCs. Either enhanced GFP siRNA (siEGFP) or *flam* siRNA (siflam) was transfected into OSCs. Nuclei are stained with DAPI (blue). Scale bar, 2 μ m.

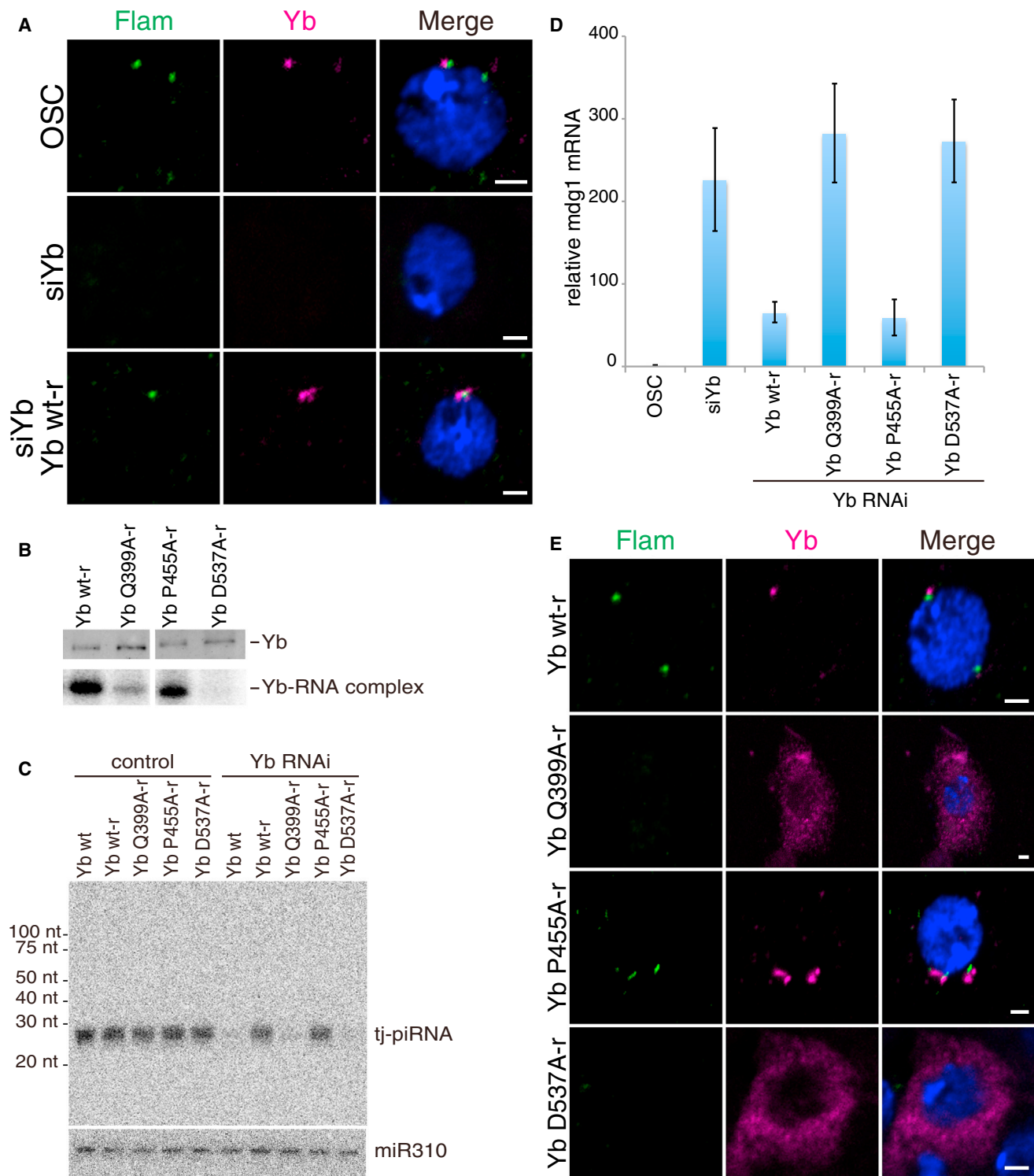


Figure 3. Yb Requirement for Flam Body and Yb Body Formation

(A) Depletion of Yb in OSCs abolishes formation of Flam bodies (green) and Yb bodies (magenta). Expression of siRNA-resistant Yb (Yb WT-r) restored the formation of both structures. Nuclei are stained with DAPI (blue). Scale bar, 2 μ m.

(B) The RNA-binding activity of Yb is abolished by either the Q399A or the D537A mutation in the Yb NTD. Western blotting using the anti-Yb antibody shows that an approximately equal amount of Yb was obtained through Yb-CLIP (top). However, the intensity of the Yb Q399A- and D537A-RNA complexes was much lower than that of the Yb P455A- and Yb WT-r-RNA complexes (bottom).

(legend continued on next page)

shown). These observations support the notion that Yb is the central player in piRNA biogenesis in OSCs; namely, Yb triggers the fabrication of two perinuclear structures, Yb bodies and Flam bodies, the hubs for piRNA maturation and piRNA intermediate concentration, respectively, in the piRNA pathway.

RNA Binding of Yb through the N-Terminal RecA-like Domain Is Required for Yb Body and Flam Body Formation

Yb shows significant similarity to DEAD-box RNA helicases such as Vasa in *Drosophila* and DDH5 and DDX18 in humans, especially in the N-terminal RecA-like domain (NTD) consisting of a Q motif and motifs I, Ia, Ib, II, and III (Figure S3D). To examine the functional involvement of the NTD of Yb in the piRNA pathway, we individually mutated highly conserved residues in Yb, Gln399, Pro455, and Asp537, to Ala. Gln399, Pro455, and Asp537 reside within the Q motif, motif Ia, and motif II, respectively (Figure S3D). In Vasa, Gln272 in the Q motif and Asp399 in motif II, which correspond to Gln399 and Asp537 in Yb, are involved in ATP binding, while Pro326 in motif Ia, which corresponds to Yb-Pro455, contributes to RNA substrate binding (Sengoku et al., 2006). ATP binding by Vasa is necessary for RNA binding (Banroques et al., 2010). Thus, we expected that the alteration of Gln399, Pro455, and Asp537 in Yb to Ala would abolish the RNA-binding function of Yb. Indeed, crosslinking and immunoprecipitation (CLIP) showed that mutation of Gln399 and Asp537 to Ala (Q399A and D537A, respectively) severely decreased the RNA-binding activity of Yb (Figure 3B). Thus, Yb is a bona fide RNA-binding protein and binds RNA substrates through the conserved NTD.

To determine if the RNA-binding activity of Yb is required in the piRNA pathway, three mutants of siRNA-resistant Yb (Q399A, P455A, and D537A), as well as Yb WT, were expressed in Yb-depleted OSCs (Figure S3E). Northern blotting showed that while the WT control Yb WT-r rescued the defect in piRNA accumulation caused by loss of Yb function, the Q399A and D537A mutants (Q399A-r and D537A-r) failed to rescue the defective phenotype (Figure 3C). The P455A mutant (P455A-r) behaved similarly to the WT control (Figure 3C), suggesting that Pro455, despite its high conservation (Figure S3D), is dispensable for piRNA biogenesis. We also examined the expression level of the *mdg1* transposon in the transfected cells, and found that Yb WT-r and P455A-r rerepressed *mdg1*, but Q399A-r and D537A-r failed to do so (Figure 3D). Q399 and D537, but not P455, in the Yb NTD are necessary for both piRNA production and piRNA-mediated transposon silencing.

We then asked if Yb WT-r and the three Yb mutants in Yb-depleted OSCs were able to restore formation of Flam bodies and Yb bodies. Yb WT-r and P455A-r were able to form Yb bodies, while Q399A-r and D537A-r were dispersed in the cytosol and did not accumulate at specific foci (Figures 3E and S3F). Correlating with this, Flam bodies appeared when

Yb WT-r and P455A-r were expressed (Figures 3E and S3F). However, the expression of Q399A-r and D537A-r did not result in the formation of Flam bodies (Figures 3E and S3F). Quantitative RT-PCR (qRT-PCR) detected *flam*-piRNA intermediates in Q399A-r- and D537A-r-expressing OSCs, where endogenous Yb had been depleted by RNAi (Figure S3G). Thus, the substitution of endogenous Yb with Q399-r or D537A-r mutant did not interfere with *flam* expression.

Yb Directly Binds *flam*-piRNA Intermediates, but Not Neighboring Protein-Coding *DIP1* Transcripts

Does endogenous Yb in OSCs indeed bind *flam* transcripts that serve as piRNA intermediates in piRNA biogenesis? To address this question, HITS-CLIP was performed in OSCs using an anti-Yb antibody. Illumina HiSeq2000 sequencing resulted in a total of 72,464,026 reads, consisting of 353,894 unique reads. We mapped these unique reads to the *Drosophila* genome, and 220,197 reads (62.2%) were mapped to a unique position. Annotation of mapped Yb-CLIP tags was similar to that of Piwi-associated piRNAs (Saito et al., 2009); over half of the reads (50.3%) were mapped to transposon regions (Figure S4A).

Further analysis of the Yb-CLIP tags showed that Yb most preferably binds transcripts from the *flam* locus among all piRNA clusters (Figure S4B). We then precisely analyzed the Yb-CLIP tags mapped to the *flam* locus. The distribution of the Yb-CLIP tags on the *flam* locus revealed that Yb in OSCs indeed associates with *flam* transcripts (Figure 4A). The Yb-CLIP tags significantly overlapped with *flam*-piRNAs associated with Piwi in OSCs (Figure 4A). By contrast, none of the Yb-CLIP tags were mapped to a neighboring coding gene, *DIP1* (Figures 4A and 4B), which is highly expressed in OSCs (Sienski et al., 2012; Cherbas et al., 2011). Yb-CLIP tag mapping to protein-coding genes that produce genic piRNAs (Saito et al., 2009) revealed that Yb almost exclusively binds the 3' UTR, but not the protein coding sequence (CDS) or 5' UTR of the transcripts (Figure S4C). The 3' UTR, but not the CDS or the 5' UTR, of genic piRNA-producing mRNAs serves as the piRNA sources (Robine et al., 2009; Saito et al., 2009). These results suggest that Yb directly, and somewhat selectively, binds piRNA intermediates in OSCs.

DISCUSSION

In this study, we visualized *flam*-piRNA intermediates in OSCs and follicle cells using RNA-FISH and EM-ISH and revealed that they concentrate at perinuclear Flam bodies. Flam bodies locate in very close proximity to Yb bodies, the sites of piRNA maturation and piRISC formation. We postulated that *flam* signals might also be detectable within Yb bodies. However, this was not the case (Figures 1B and S1A). The simplest explanation for this observation is that piRNA processing at Yb bodies occurs so quickly, and the processed piRNAs localize to the nucleus as

(C) Expression of Yb WT-r and P455A-r, but not Q399A-r and D537A-r, rescued the defect in piRNA accumulation in Yb-depleted OSCs. A piRNA arising from a *traffic jam* (*tj*) gene (Saito et al., 2009) was visualized by northern blotting using a specific DNA probe. miR310, loading control.

(D) Expression of Yb WT-r and P455A-r rerepressed the *mdg1* transposon in Yb-depleted OSCs, but expression of Q399A-r or D537A-r could not.

(E) Mutation of Q399A and D537A in Yb abolished Flam body (green) and Yb body (magenta) formation in OSCs. Endogenous Yb was depleted by RNAi. Nuclei are stained with DAPI (blue). Scale bar, 2 μ m.

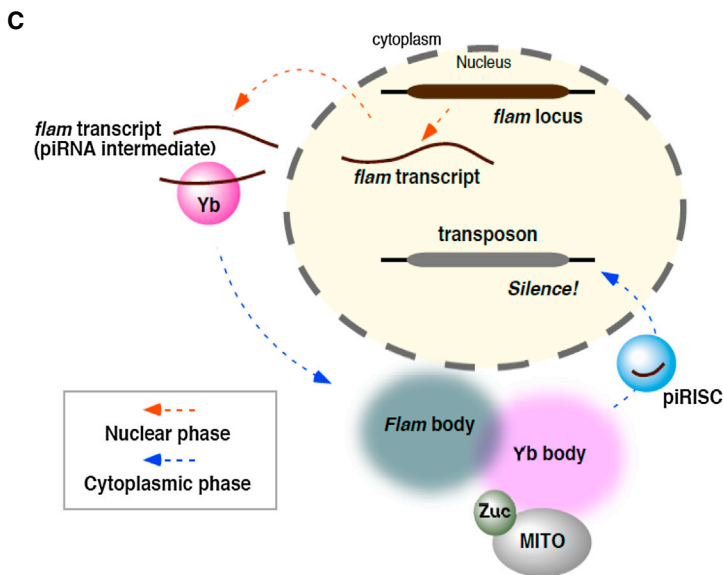
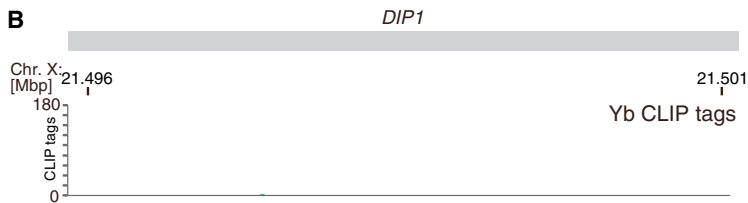
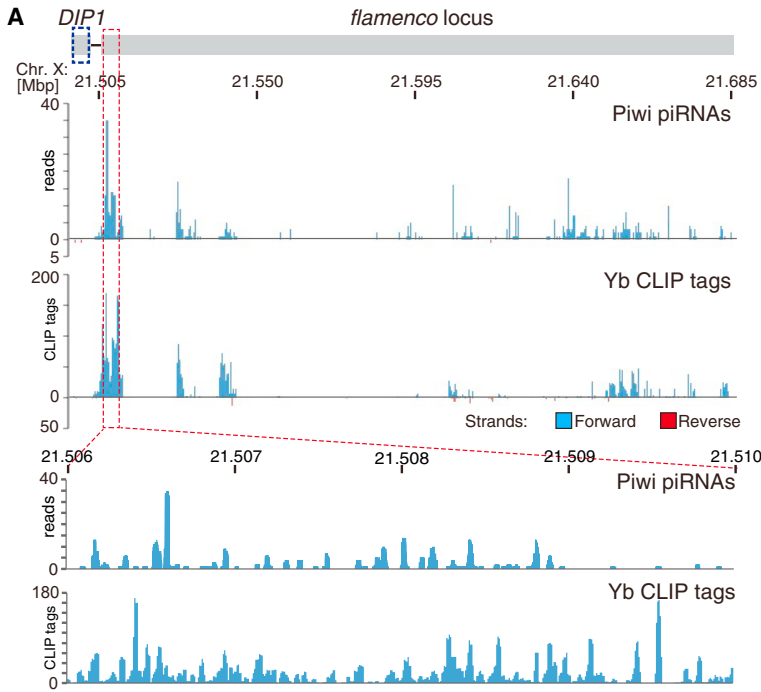


Figure 4. Yb Binds *flam* Transcripts, but Not *DIP1* mRNAs, In Vivo

(A) Mapped Piwi-piRNA reads and Yb-CLIP tags on the *DIP1* coding and *flam* cluster region. Forward reads are shown in blue, and reverse reads are shown in red. The number on the side of tracks denotes the number of reads in each position. Genomic coordinates are marked above the tracks. The bottom panel shows a further zoom-in view of sequences around the region where the RNA-FISH probe was designed to bind.

(B) A further zoom-in view of sequences of the *DIP1* gene in (A) (boxed by a dotted blue line).

(C) A new model for primary piRNA biogenesis in OSCs. The transcription and nuclear export of the transcripts are considered to be the “nuclear phase” of piRNA biogenesis. The *flam* transcripts become *flam*-piRNA intermediates by “shortening” in either the nucleus or the cytoplasm. The mechanism underlying the shortening process remains unknown. Yb binds piRNA intermediates in the cytoplasm and locates to Flam bodies. piRNA intermediates are further processed to mature piRNAs at Yb bodies with the help of Zuc on mitochondria (MITO) and loaded onto Piwi, giving rise to the piRISC. The piRISC is imported to the nucleus, where the RNP complex exerts its function: transcriptional silencing of transposons. Yb-piRNA intermediate association, piRNA maturation, and piRISC assembly are considered to be the “cytoplasmic phase” of piRNA biogenesis. Components of Yb bodies include Yb, Armi, Vret, SoYb, and Shu, all of which are required for piRNA biogenesis and piRISC formation in OSCs.

piRISCs so immediately, that the *flam* signal at Yb bodies was below the level of detection at Yb bodies.

In Zuc-depleted cells, *flam* transcripts were detected predominantly as *flam*-piRNA intermediates, being several hundred to 4,000 nt in length (Figures 2C and S2A), while the full transcriptional unit of *flam* is estimated to be over 180 kb (Brennecke et al., 2007; Malone et al., 2009). Both Yb body and Flam body formation require Yb, or more precisely, its RNA-binding activity through its NTD (Figures 3B, 3E, and S3F). Yb binds *flam*-piRNA intermediates directly (Figure 4A). Based on these findings, we propose a new model for primary piRNA biogenesis in ovarian soma (Figure 4C), in which the association of Yb with piRNA intermediates, which most likely occurs in the cytoplasm because Yb is a cytoplasmic protein (Olivieri et al., 2010; Saito et al., 2010), is the initiation point of the cytoplasmic phase of piRNA biogenesis. This follows the nuclear phase of piRNA biogenesis: *flam* transcription and nuclear export of *flam* transcripts through the nuclear pores. *flam* transcription is initiated by RNA polymerase II and requires the transcriptional factor Cubitus interruptus (Goriaux et al., 2014). However, it is not known by which export factors and in what lengths the *flam* transcripts are exported from the nucleus. Further investigation will be required for a detailed understanding of the nuclear phase of piRNA biogenesis.

The locations of the genomic *flam* loci in the nucleus and Flam bodies do not seem to be arranged to be close to each other, meaning that the *flam* transcripts move a long distance to arrive at Flam bodies (Figure 4C). Do the *flam* transcripts move within the nucleus to get closer to Flam bodies before export to the cytoplasm? Alternatively, does nuclear export occur first and then *flam* transcripts are localized to Flam bodies? Yb localization in the cytoplasm seems to be so dynamic that a point mutation in Yb that disrupts the RNA-binding capacity of Yb drastically changes the subcellular localization of Yb, causing it to be scattered evenly in the cytosol (Figures 3E and S3F). Thus, the latter scenario appears more likely, in which Yb plays a crucial role; upon nuclear export, Yb captures *flam* transcripts through direct binding and localizes them, as *flam*-piRNA intermediates, to Flam bodies. Flam body formation depends on the RNA-binding activity of Yb, a cytoplasmic protein (Olivieri et al., 2010; Saito et al., 2010); this notion further supports the idea that Flam bodies are cytoplasmic structures.

Unlike *flam* transcripts, *DIP1* mRNAs were virtually undetectable in Yb-CLIP tags (Figures 4A and 4B), although the *DIP1* protein-coding gene and the *flam* piRNA cluster are neighbors on chromosome X (Figure 1A) and *DIP1* is expressed in OSCs. We looked carefully at the sequences of Yb-CLIP tags but found no obvious consensus sequences. Yb may recognize binding substrates owing to higher-order structures.

Immunoelectron microscopy using an anti-Yb antibody showed that Yb bodies are often attached to mitochondria, to which Zuc endoribonuclease, the piRNA intermediate processor, anchors on the surface to face into cytoplasmic Yb bodies (Figure 1D). This peculiar spatial arrangement of Zuc and Yb bodies, along with Flam bodies, integrates all the ingredients necessary for primary piRNA production locally, enhancing the rates of piRISC assembly. Another virtue of this perinuclear

arrangement is that it enables assembled piRISCs to be immediately imported into the nucleus, where the RNP complex (i.e., the PIWI-piRNA complex) exerts its nuclear-specific function of silencing transposon transcription (Sienski et al., 2012). How does Yb decide where within the perinuclear region to integrate all the materials necessary for primary piRNA biogenesis? Reconstitution of the whole machinery in, for instance, nongonadal somatic Schneider2 cells, in which no primary piRNAs are otherwise expressed, might address this fundamental question.

EXPERIMENTAL PROCEDURES

Detailed procedures are provided in [Supplemental Experimental Procedures](#).

Drosophila Strains

Yellow white (*y w*) and the *flam* [*KG00476*] and the *fs(1)Yb[72]* alleles were used. Fly stocks were maintained at 25°C.

Cell Culture and RNAi

OSCs were grown in OSC medium prepared from Shields and Sang M3 Insect Medium (Sigma) supplemented with 0.6 mg/ml glutathione, 10% fetal bovine serum, 10 mU/ml insulin, and 10% fly extract. RNAi was performed using RNA oligos shown in [Table S1](#).

Production of Anti-Yb Antibodies

Monoclonal antibodies against Yb were raised primarily as described previously (Ohtani et al., 2013). A recombinant protein consisting of glutathione S-transferase and the N-terminal region of Yb (200 amino acids) was purified from *E. coli* and injected into mice.

RNA-FISH

The fluorescein isothiocyanate (FITC)- and digoxigenin-labeled RNA probes were prepared using RNA labeling mixture (Roche) and SP6RNA polymerase (Roche) according to the manufacturer's instructions. To prepare a probe specific for the *flam* locus, OSC genomic DNA was used as a template for PCR. The primers used for PCR are indicated in [Table S1](#). In situ hybridization was carried out essentially as described previously (Sone et al., 2007).

DNA-FISH

Digoxigenin- or biotin-labeled DNA probes were prepared using Nick Translation Mix (Roche) according to the manufacturer's instructions. To prepare the probes, bacterial artificial chromosome clones DME1-021J16 (upstream of the *flam* locus) and DME1-014M21 (downstream of the *flam* locus), were used as templates. OSCs were treated with ice-cold 0.75 M KCl for 5 min and then, after resuspending in acetic acid-methanol (1:3), spread onto slides. The slides were treated essentially according to the procedures of Masumoto et al. (Masumoto et al., 1989).

Immunofluorescence

Immunofluorescence was performed primarily as described previously (Ohtani et al., 2013; Saito et al., 2009).

Body Counting

Confocal images of immunofluorescence were transferred to the Columbus System (PerkinElmer Japan) and analyzed by Building Block (PerkinElmer Japan). Nuclei were masked and then perinuclear signals for Yb bodies and Flam bodies were detected.

Electron Microscopy In Situ Hybridization

OSCs were fixed with 4% paraformaldehyde (PFA) in 0.1 M PBS (pH 7.4) overnight and then washed with RNase-free PBS. The samples were hybridized with FITC-conjugated specific RNA probe, except that 0.5% Triton X-100 was used for 5 min. Samples were incubated with a primary rabbit anti-FITC (1:500) antibody and then washed in 0.1 M phosphate buffer (PB) containing

0.005% saponin. Samples were incubated for 24 hr at 4°C with nanogold-conjugated anti-rabbit secondary antibody (1:100, Invitrogen).

Immunoelectron Microscopy

OSCs were fixed with 0.1% glutaraldehyde and 4% PFA in 0.1 M PBS, followed by incubation with 5% Block Ace containing 0.1% saponin in 0.1 M PB. The cells were stained with anti-Yb antibody (1:250) and nanogold-conjugated anti-mouse secondary antibody (1:100, Invitrogen).

Western Blot Analysis

Western blotting was performed primarily as described previously (Miyoshi et al., 2005).

Northern Blot Analysis

For *flam* transcript detection, total RNAs were isolated from OSC using ISOGEN (Nippon Gene). Hybridization was performed with random-labeled antisense oligodeoxynucleotide probe. Small RNAs were detected essentially as previously described (Saito et al., 2009).

Plasmid Construction

An expression vector for myc-Yb WT was generated by inserting the WT Yb coding region into the pAcM vector (Saito et al., 2009). myc-Yb-r was constructed as essentially described previously (Saito et al., 2010). Primers are listed in Table S1.

qRT-PCR Analysis

Reverse transcription was performed using a PrimerScript RT Master Mix (TaKaRa). The resulting cDNAs were amplified using a LightCycler 480 Real-Time PCR Instrument II (Roche) with SYBR Premix Ex Taq (TaKaRa). The primers used are listed in Table S1.

CLIP

CLIP was performed primarily as described previously (Jaskiewicz et al., 2012). Anti-Yb was used to immunopurify Yb from OSCs after irradiation by UV (254 nm) for crosslinking.

Bioinformatic Analysis

The Yb-CLIP library was sequenced using the Illumina HiSeq2000 platform according to the manufacturer's instructions. The average base-wise quality was checked, and those that passed quality control were subjected to analyses.

ACCESSION NUMBERS

Yb-CLIP tag sequencing data have been deposited in the Gene Expression Omnibus under the accession number GSE54875.

SUPPLEMENTAL INFORMATION

Supplemental Information includes Supplemental Experimental Procedures, four figures, and one table and can be found with this article online at <http://dx.doi.org/10.1016/j.celrep.2014.05.043>.

AUTHOR CONTRIBUTIONS

M.Y., H.I., S.N., Y.W.I., S.S., M.K.K., and K.S. designed and performed experiments and helped write the manuscript. H.O. supervised electron microscopic experiments. H.S. and M.C.S. conceived the study and wrote the manuscript.

ACKNOWLEDGMENTS

We thank H. Masumoto for technical advice and Y. Iyoda, H. Kotani, T. Yano, and T. Nagai for technical assistance. We also thank M. Isogai and M. Shimura (PerkinElmer Japan) for their assistance with fluorescence quantification. This work was supported by CREST-JST (to M.C.S.), by a Grant-in-Aid for Scientific Research from MEXT (to S.N., Y.W.I., S.S., K.S., H.O., H.S. and M.C.S.), and

by a Grant-in-Aid for the Global COE program from MEXT to Keio University (H.S. and H.O.).

Received: December 16, 2013

Revised: April 9, 2014

Accepted: May 21, 2014

Published: June 19, 2014

REFERENCES

- Aravin, A.A., Hannon, G.J., and Brennecke, J. (2007). The Piwi-piRNA pathway provides an adaptive defense in the transposon arms race. *Science* *318*, 761–764.
- Banroques, J., Doère, M., Dreyfus, M., Linder, P., and Tanner, N.K. (2010). Motif III in superfamily 2 “helicases” helps convert the binding energy of ATP into a high-affinity RNA binding site in the yeast DEAD-box protein Ded1. *J. Mol. Biol.* *396*, 949–966.
- Brennecke, J., Aravin, A.A., Stark, A., Dus, M., Kellis, M., Sachidanandam, R., and Hannon, G.J. (2007). Discrete small RNA-generating loci as master regulators of transposon activity in *Drosophila*. *Cell* *128*, 1089–1103.
- Cherbas, L., Willingham, A., Zhang, D., Yang, L., Zou, Y., Eads, B.D., Carlson, J.W., Landolin, J.M., Kapranov, P., Dumais, J., et al. (2011). The transcriptional diversity of 25 *Drosophila* cell lines. *Genome Res.* *21*, 301–314.
- Choi, S.Y., Huang, P., Jenkins, G.M., Chan, D.C., Schiller, J., and Frohman, M.A. (2006). A common lipid links Mfn-mediated mitochondrial fusion and SNARE-regulated exocytosis. *Nat. Cell Biol.* *8*, 1255–1262.
- Cook, H.A., Koppetsch, B.S., Wu, J., and Theurkauf, W.E. (2004). The *Drosophila* SDE3 homolog armitage is required for oskar mRNA silencing and embryonic axis specification. *Cell* *116*, 817–829.
- Dennis, C., Zanni, V., Brasset, E., Eymery, A., Zhang, L., Mteirek, R., Jensen, S., Rong, Y.S., and Vaury, C. (2013). “Dot COM”, a nuclear transit center for the primary piRNA pathway in *Drosophila*. *PLoS ONE* *8*, e72752.
- Dönertas, D., Siensi, G., and Brennecke, J. (2013). *Drosophila* Gtsf1 is an essential component of the Piwi-mediated transcriptional silencing complex. *Genes Dev.* *27*, 1693–1705.
- Goriaux, C., Dessel, S., Renaud, Y., Vaury, C., and Brasset, E. (2014). Transcriptional properties and splicing of the *flamenco* piRNA cluster. *EMBO Rep.* *15*, 411–418.
- Gunawardane, L.S., Saito, K., Nishida, K.M., Miyoshi, K., Kawamura, Y., Nagami, T., Siomi, H., and Siomi, M.C. (2007). A slicer-mediated mechanism for repeat-associated siRNA 5' end formation in *Drosophila*. *Science* *315*, 1587–1590.
- Haase, A.D., Fenoglio, S., Muerdter, F., Guzzardo, P.M., Czech, B., Pappin, D.J., Chen, C., Gordon, A., and Hannon, G.J. (2010). Probing the initiation and effector phases of the somatic piRNA pathway in *Drosophila*. *Genes Dev.* *24*, 2499–2504.
- Handler, D., Olivieri, D., Novatchkova, M., Gruber, F.S., Meixner, K., Mechtler, K., Stark, A., Sachidanandam, R., and Brennecke, J. (2011). A systematic analysis of *Drosophila* TUDOR domain-containing proteins identifies Vreteno and the Tdrd12 family as essential primary piRNA pathway factors. *EMBO J.* *30*, 3977–3993.
- Ipsaro, J.J., Haase, A.D., Knott, S.R., Joshua-Tor, L., and Hannon, G.J. (2012). The structural biochemistry of Zucchini implicates it as a nuclease in piRNA biogenesis. *Nature* *491*, 279–283.
- Ishizu, H., Siomi, H., and Siomi, M.C. (2012). Biology of PIWI-interacting RNAs: new insights into biogenesis and function inside and outside of germlines. *Genes Dev.* *26*, 2361–2373.
- Jaskiewicz, L., Bilen, B., Hausser, J., and Zavolan, M. (2012). Argonaute CLIP—a method to identify *in vivo* targets of miRNAs. *Methods* *58*, 106–112.
- Juliano, C., Wang, J., and Lin, H. (2011). Uniting germline and stem cells: the function of Piwi proteins and the piRNA pathway in diverse organisms. *Annu. Rev. Genet.* *45*, 447–469.

- Khurana, J.S., and Theurkauf, W. (2010). piRNAs, transposon silencing, and *Drosophila* germline development. *J. Cell Biol.* *191*, 905–913.
- Malone, C.D., Brennecke, J., Dus, M., Stark, A., McCombie, W.R., Sachidanandam, R., and Hannon, G.J. (2009). Specialized piRNA pathways act in germline and somatic tissues of the *Drosophila* ovary. *Cell* *137*, 522–535.
- Masumoto, H., Sugimoto, K., and Okazaki, T. (1989). Alphoid satellite DNA is tightly associated with centromere antigens in human chromosomes throughout the cell cycle. *Exp. Cell Res.* *181*, 181–196.
- Mével-Ninio, M., Pelisson, A., Kinder, J., Campos, A.R., and Bucheton, A. (2007). The *flamenco* locus controls the gypsy and ZAM retroviruses and is required for *Drosophila* oogenesis. *Genetics* *175*, 1615–1624.
- Miyoshi, K., Tsukumo, H., Nagami, T., Siomi, H., and Siomi, M.C. (2005). Slicer function of *Drosophila* Argonautes and its involvement in RISC formation. *Genes Dev.* *19*, 2837–2848.
- Muerdter, F., Guzzardo, P.M., Gillis, J., Luo, Y., Yu, Y., Chen, C., Fekete, R., and Hannon, G.J. (2013). A genome-wide RNAi screen draws a genetic framework for transposon control and primary piRNA biogenesis in *Drosophila*. *Mol. Cell* *50*, 736–748.
- Nishimasu, H., Ishizu, H., Saito, K., Fukuhara, S., Kamatani, M.K., Bonnefond, L., Matsumoto, N., Nishizawa, T., Nakanaga, K., Aoki, J., et al. (2012). Structure and function of Zucchini endoribonuclease in piRNA biogenesis. *Nature* *491*, 284–287.
- Ohtani, H., Iwasaki, Y.W., Shibuya, A., Siomi, H., Siomi, M.C., and Saito, K. (2013). DmGTSF1 is necessary for Piwi-piRISC-mediated transcriptional transposon silencing in the *Drosophila* ovary. *Genes Dev.* *27*, 1656–1661.
- Olivieri, D., Sykora, M.M., Sachidanandam, R., Mechtler, K., and Brennecke, J. (2010). An in vivo RNAi assay identifies major genetic and cellular requirements for primary piRNA biogenesis in *Drosophila*. *EMBO J.* *29*, 3301–3317.
- Olivieri, D., Senti, K.A., Subramanian, S., Sachidanandam, R., and Brennecke, J. (2012). The cochaperone shutdown defines a group of biogenesis factors essential for all piRNA populations in *Drosophila*. *Mol. Cell* *47*, 954–969.
- Pillai, R.S., and Chuma, S. (2012). piRNAs and their involvement in male germline development in mice. *Dev. Growth Differ.* *54*, 78–92.
- Qi, H., Watanabe, T., Ku, H.Y., Liu, N., Zhong, M., and Lin, H. (2011). The Yb body, a major site for Piwi-associated RNA biogenesis and a gateway for Piwi expression and transport to the nucleus in somatic cells. *J. Biol. Chem.* *286*, 3789–3797.
- Robine, N., Lau, N.C., Balla, S., Jin, Z., Okamura, K., Kuramochi-Miyagawa, S., Blower, M.D., and Lai, E.C. (2009). A broadly conserved pathway generates 3'UTR-directed primary piRNAs. *Curr. Biol.* *19*, 2066–2076.
- Saito, K., Inagaki, S., Mituyama, T., Kawamura, Y., Ono, Y., Sakota, E., Kotani, H., Asai, K., Siomi, H., and Siomi, M.C. (2009). A regulatory circuit for *piwi* by the large Maf gene *traffic jam* in *Drosophila*. *Nature* *461*, 1296–1299.
- Saito, K., Ishizu, H., Komai, M., Kotani, H., Kawamura, Y., Nishida, K.M., Siomi, H., and Siomi, M.C. (2010). Roles for the Yb body components Armitage and Yb in primary piRNA biogenesis in *Drosophila*. *Genes Dev.* *24*, 2493–2498.
- Sengoku, T., Nureki, O., Nakamura, A., Kobayashi, S., and Yokoyama, S. (2006). Structural basis for RNA unwinding by the DEAD-box protein *Drosophila* Vasa. *Cell* *125*, 287–300.
- Sienski, G., Dönertas, D., and Brennecke, J. (2012). Transcriptional silencing of transposons by Piwi and maelstrom and its impact on chromatin state and gene expression. *Cell* *151*, 964–980.
- Siomi, M.C., Sato, K., Pezic, D., and Aravin, A.A. (2011). PIWI-interacting small RNAs: the vanguard of genome defence. *Nat. Rev. Mol. Cell Biol.* *12*, 246–258.
- Sone, M., Hayashi, T., Tarui, H., Agata, K., Takeichi, M., and Nakagawa, S. (2007). The mRNA-like noncoding RNA Gomafu constitutes a novel nuclear domain in a subset of neurons. *J. Cell Sci.* *120*, 2498–2506.
- Szakmary, A., Reedy, M., Qi, H., and Lin, H. (2009). The Yb protein defines a novel organelle and regulates male germline stem cell self-renewal in *Drosophila melanogaster*. *J. Cell Biol.* *185*, 613–627.
- Zamparini, A.L., Davis, M.Y., Malone, C.D., Vieira, E., Zavadil, J., Sachidanandam, R., Hannon, G.J., and Lehmann, R. (2011). Vreteno, a gonad-specific protein, is essential for germline development and primary piRNA biogenesis in *Drosophila*. *Development* *138*, 4039–4050.

Supplemental Information

Yb integrates piRNA intermediates and processing factors into perinuclear bodies to enhance piRISC assembly

Yukiko Murota^{1,2*}, Hirotugu Ishizu^{3*}, Shinichi Nakagawa⁴, Yuka W. Iwasaki², Shinsuke Shibata⁵, Mihar K. Kamatani², Kuniaki Saito², Hideyuki Okano⁵, Haruhiko Siomi² and Mikiko C. Siomi^{2,3+}

¹Institute for Genome Research, University of Tokushima, Tokushima, Japan, ²Division of Molecular Biology, Keio University School of Medicine, Tokyo, Japan, ³Department of Biophysics and Biochemistry, Graduate School of Science, The University of Tokyo, Tokyo, Japan, ⁴RIKEN, Wako, Saitama, Japan, ⁵Division of Biomedical Physiology, Keio University School of Medicine, Tokyo, Japan

*These authors contributed equally to this work

+Corresponding author

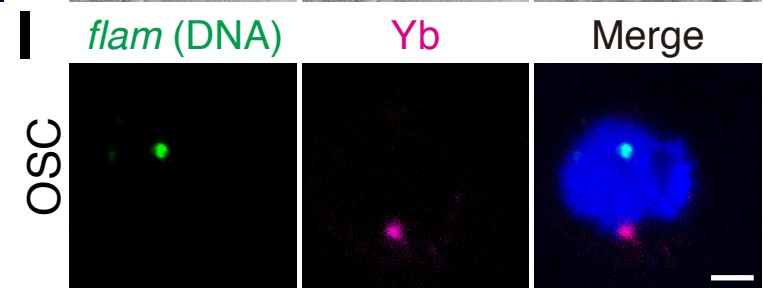
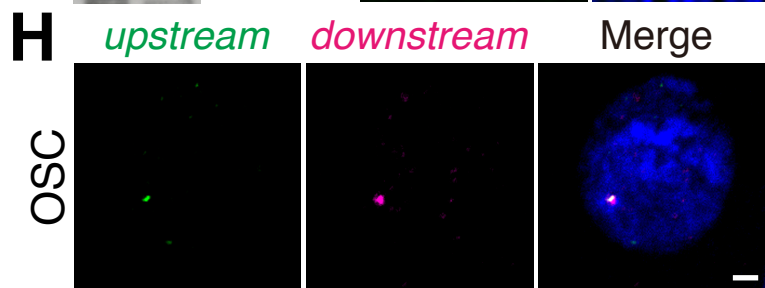
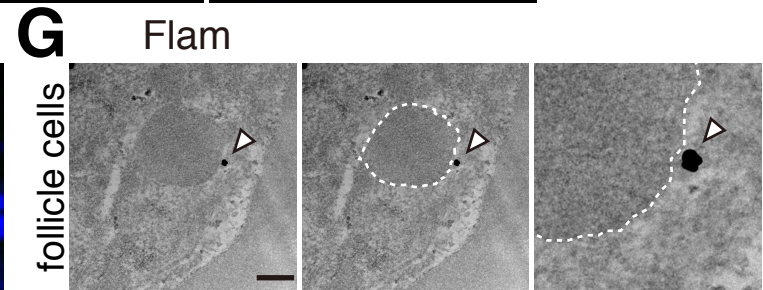
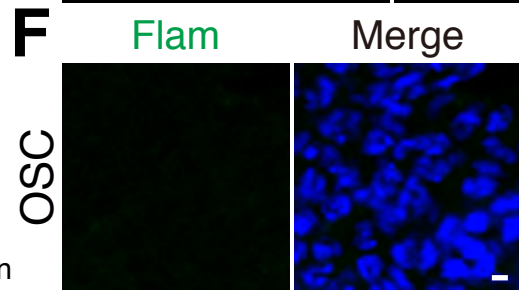
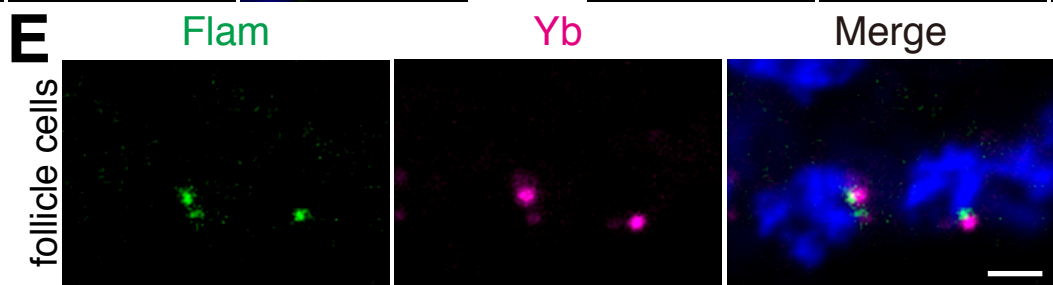
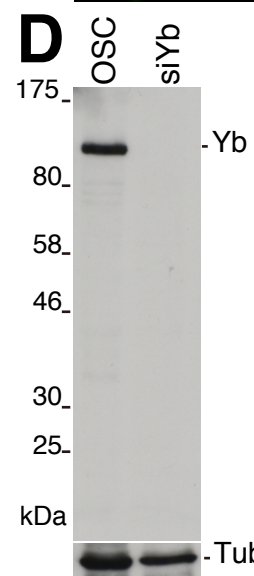
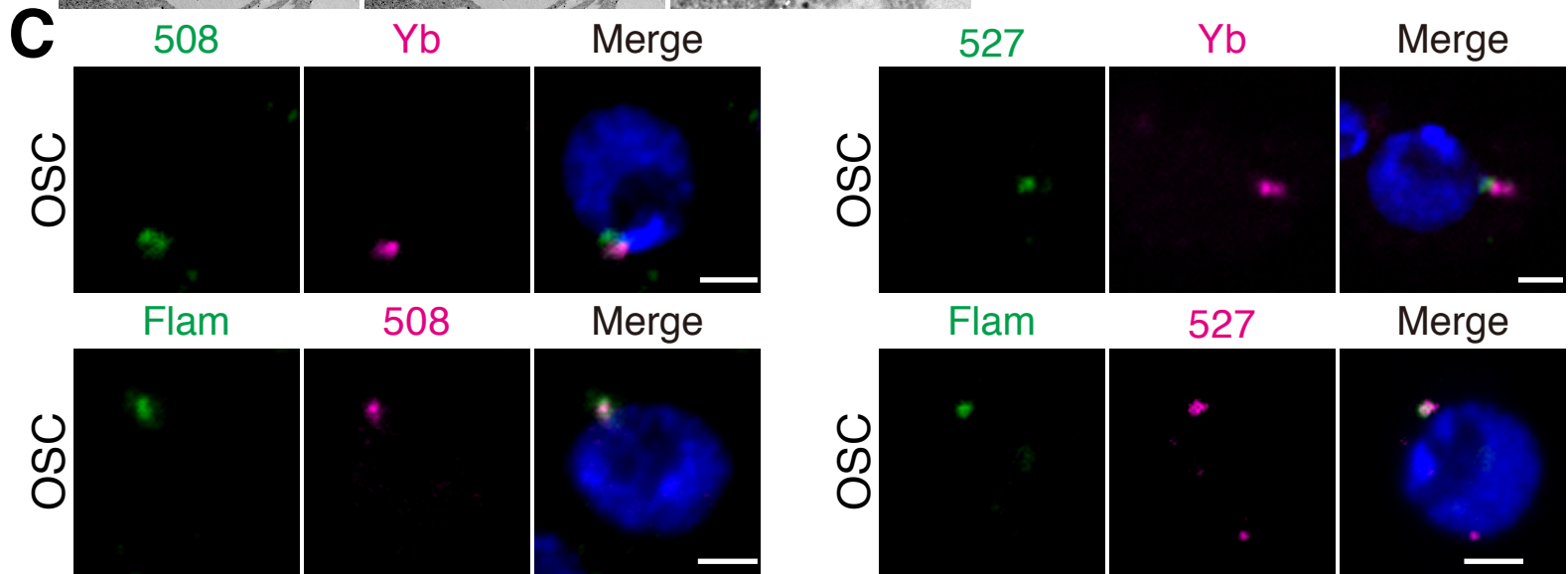
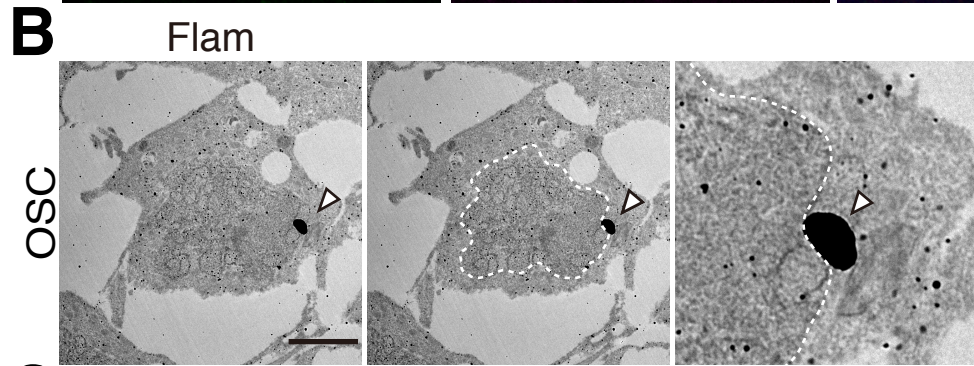
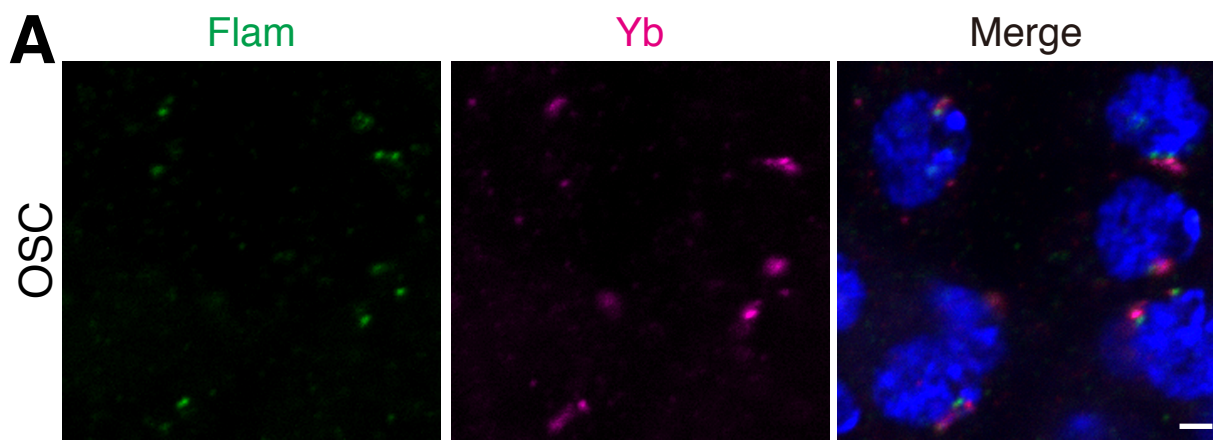
Contents:

Figures S1-S4

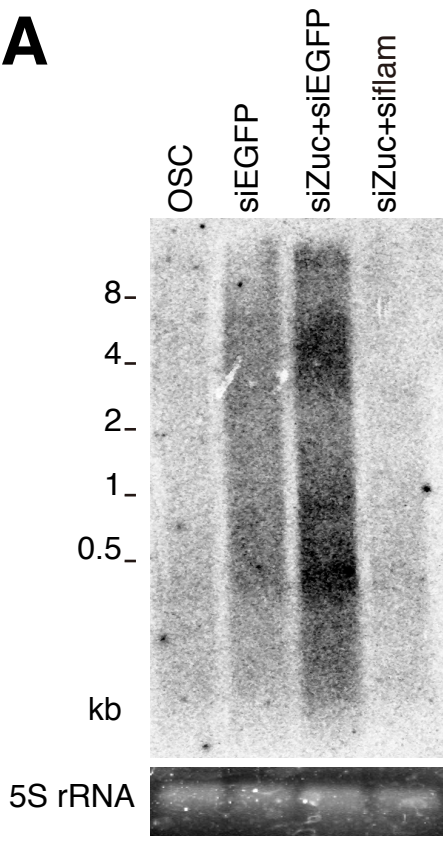
Table S1

Supplemental Experimental Procedures

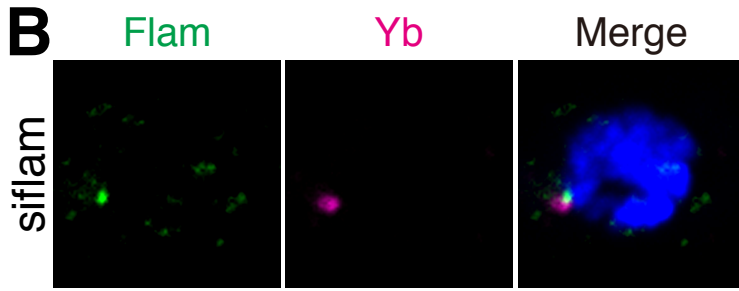
Supplemental References



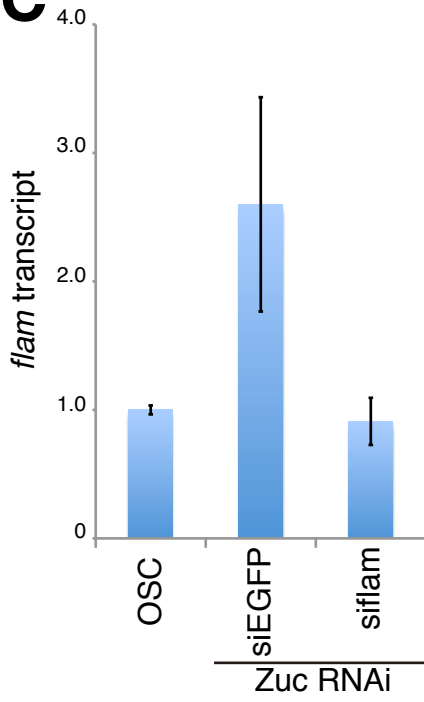
A

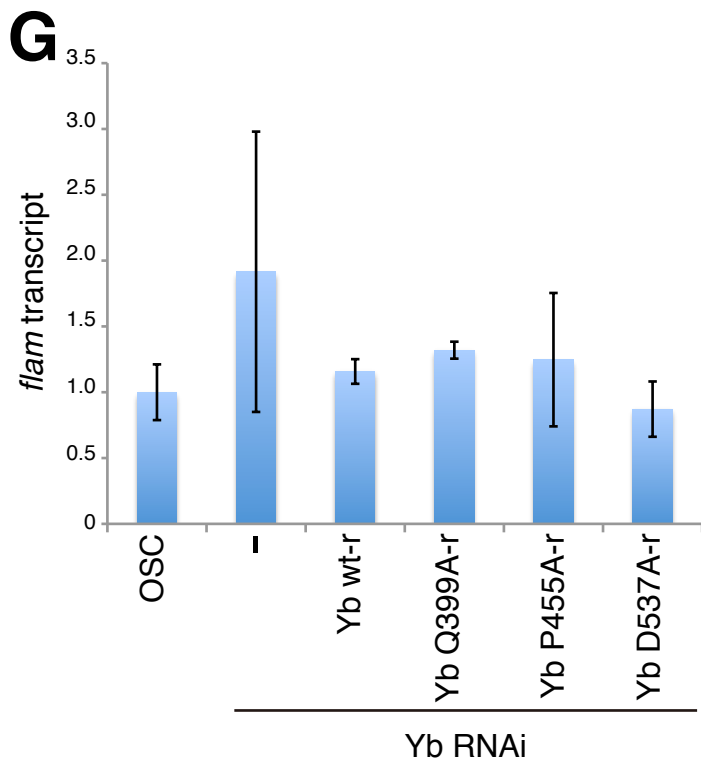
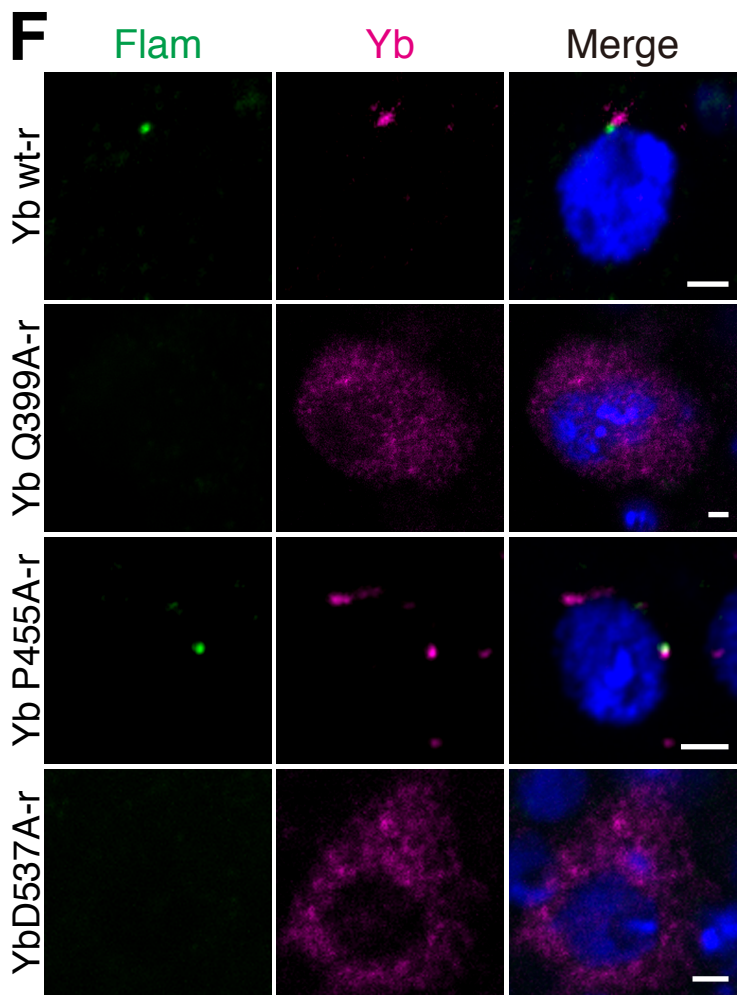
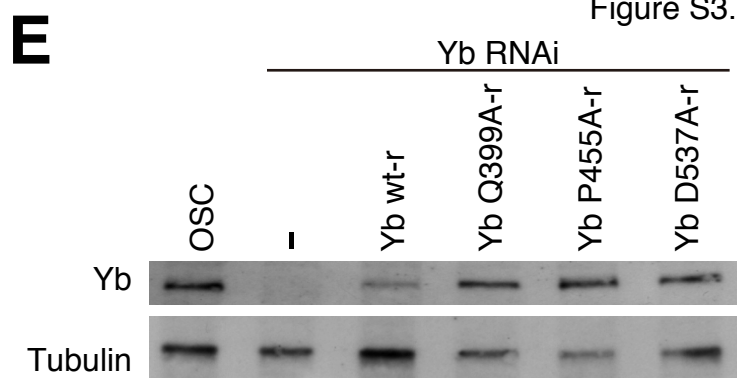
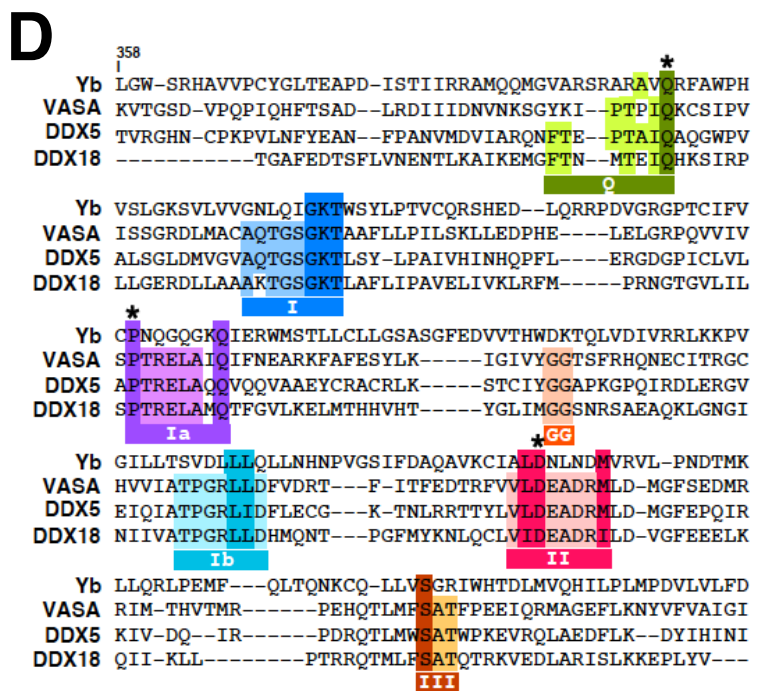
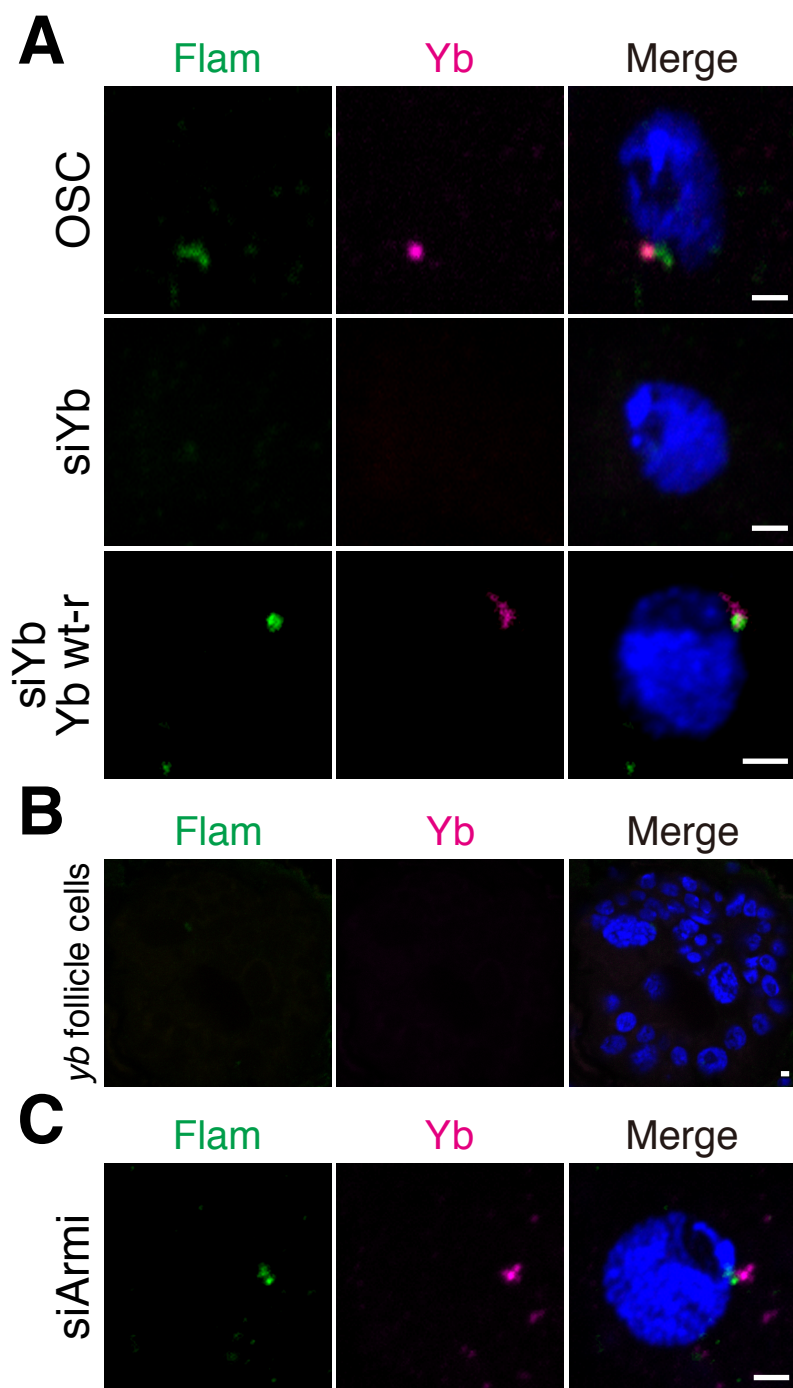


B

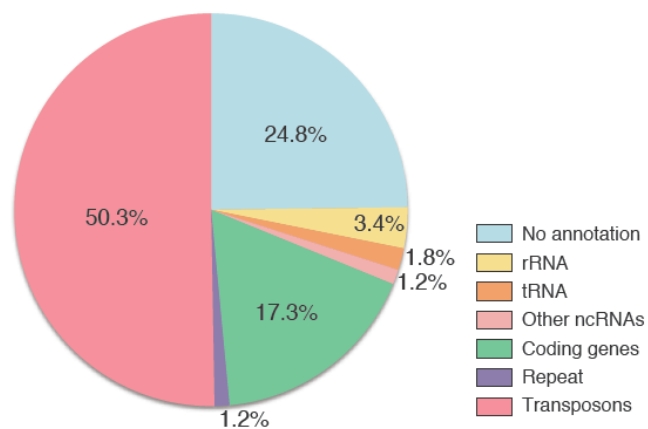


C





A



B

Cluster Name	Chromosome	Start	Stop	Size	Piwi-piRNA reads (Saito et al)	Unique Yb-CLIP tags	
piRNA_cluster_01	chr2R	2144349	2386719	242370	2	30	42AB
piRNA_cluster_02	chrX	21392175	21431907	39732	29	286	
piRNA_cluster_05	chr2L	20148259	20227581	79322	0	8	
piRNA_cluster_06	chr3L	23273964	23314199	40235	0	30	
piRNA_cluster_07	chrX	21505666	21684449	178783	1338	7568	flamenco
piRNA_cluster_08	chrX	21759393	21844063	84670	0	126	
piRNA_cluster_10	chr3LHet	1402377	1557939	155562	1	49	
piRNA_cluster_11	chr3LHet	2011004	2180268	169264	0	24	
piRNA_cluster_12	chr3LHet	238123	332969	94846	0	23	
piRNA_cluster_13	chr3RHet	2033725	2108757	75032	0	13	
piRNA_cluster_14	chrU	964336	1041768	77432	68	3408	
piRNA_cluster_15	chrU	3113117	3137249	24132	14	627	
piRNA_cluster_16	chr3R	8293500	8328300	34800	0	2	
piRNA_cluster_17	chr3LHet	773130	897972	124842	0	34	
piRNA_cluster_18	chr2RHet	2820000	2898450	78450	4	43	

C

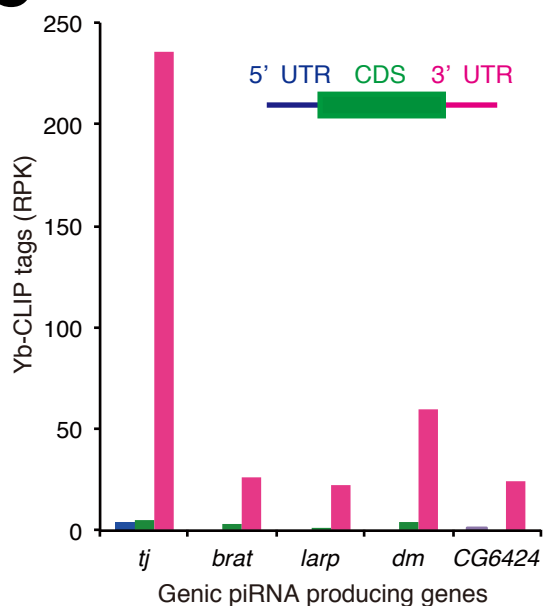


Figure S1, related to Figure 1. Flam bodies and Yb bodies in OSC and follicle cells. (A) Flam bodies (green) and Yb bodies (magenta) in OSC are visualized by RNA-FISH and immunofluorescence using anti-Yb antibody, respectively. Nuclei are stained with DAPI (blue). Scale bar; 2 μ m. (B) EM-ISH shows that Flam body is cytoplasmic. A white dot line represents a nucleus. Scale bar; 2 μ m. (C) Upper panel: *flam*/*COM* riboprobes (508 and 527) (Dennis et al., 2013) and anti-Yb antibody were used to visualize Flam bodies (green) and Yb bodies (magenta), respectively, in OSC. Lower panel: RNA-FISH shows that 508 and 527 signals (magenta) coincide with the *flam* signals (green). Nuclei are stained with DAPI (blue). Scale bar; 2 μ m. (D) Western blotting shows the specificity of the anti-Yb antibody raised in this study. OSC lysates prepared before and after treatment with Yb siRNA (siYb) were used. (E) Flam bodies (green) and Yb bodies (magenta) were detected in follicular cells in the ovaries. Nuclei are stained with DAPI (blue). Scale bar; 2 μ m. (F) Flam bodies (green) in *flam* mutant follicle cells. DAPI stained the nuclei (blue). Scale bar; 2 μ m. (G) EM-ISH shows that Flam body is cytoplasmic in follicle cells. A white dot line represents a nucleus. Scale bar; 0.2 μ m. (H) DNA-FISH was performed on OSC using two probes recognizing upstream (green) and downstream (magenta) regions of the *flam* locus on chromosome X. The upstream and downstream signals overlapped. The nucleus is stained with DAPI (blue). Scale bar; 2 μ m. (I) Visualization of the *flam* loci (green) in the nucleus and Yb body (magenta) in the cytoplasm in OSC. The nucleus is stained with DAPI (blue). Scale bar; 2 μ m.

Figure S2, related to Figure 2. Effects of siZuc and siflam transfection in OSC. (A) Northern blotting shows that transfection of OSC with Zuc siRNA (siZuc) induces aberrant accumulation of *flam*-piRNA intermediates in OSC. Probes targeting the 508 RNA-FISH probe region (Dennis et al., 2013) were used. EGFP siRNA (siEGFP) was used as a negative control. 5S rRNA (loading control) was visualized by EtBr staining. (B) Treatment with siflam barely affects Flam body formation in OSC. (C) Treatment with siflam down-regulated the levels of *flam* transcripts in Zuc-depleted OSC, which now returned to normal as in naïve OSC. EGFP siRNA (siEGFP) was used as a control. The experiments were carried out three times.

Figure S3, related to Figure 3. Requirement of Yb in the primary piRNA pathway in OSC. (A) Depletion of Yb in OSC disrupted Flam bodies (green) and Yb bodies

(magenta). Expression of siRNA-resistant Yb (Yb wt-r) restored the formation of both structures. Nuclei are stained with DAPI (blue). Scale bar; 2 μ m. **(B)** Flam bodies (green) and Yb bodies (magenta) are not detected in *yb* mutant follicle cells. Nuclei are stained with DAPI (blue). Scale bar; 2 μ m. **(C)** Depletion of Armi in OSC barely affected formation of Flam bodies (green) and Yb bodies (magenta). The nucleus is stained with DAPI (blue). Scale bar; 2 μ m. **(D)** Amino acid sequence alignment of the NTD of DEAD-box proteins, Vasa, DDX5 and DDH18, and Yb. Highly conserved amino acids are boxed. Three amino acids mutated to alanine are indicated with asterisks. **(E)** Western blotting shows that treatment of OSC by Yb siRNA (siYb) abolished the expression of Yb. The expression levels of Yb wt-r, Yb Q399A-r, Yb P455A-r and D537A-r in Yb-depleted OSC are examined. Tubulin was used as a loading control. **(F)** Q399A and D537A mutations in Yb abolish formation of Flam bodies (green) and Yb bodies (magenta) in OSC. Endogenous Yb was depleted by RNAi. The nuclei are stained with DAPI (blue). Scale bar; 2 μ m. **(G)** qRT-PCR detects *flam* transcripts in Yb wt-r, Yb Q399A-r, Yb P455A-r and Yb D537A-r expressing OSC, where endogenous Yb had been depleted by RNAi. The experiments were carried out three times.

Figure S4, related to Figure 4. Yb-CLIP analyses **(A)** Annotation of *Drosophila* genomic regions where Yb-CLIP tags were mapped. **(B)** The table showing the number of Yb-CLIP tags and Piwi-piRNA reads (Saito et al., 2009) mapped to each of the piRNA clusters. Genomic positions of piRNA clusters were obtained from previous publication (Malone et al., 2009). The clusters harboring over 10 Piwi-piRNA reads are highlighted in red. **(C)** The bar graph shows the enrichment of Yb-CLIP tags in the 3' UTR of top 5 genic piRNA producing transcripts (obtained from Robine et al, 2009). Read per kilobase (RPK) values of Yb-CLIP tags are shown for 5' UTR (blue), CDS (green), and 3' UTR (pink) of each transcript.

Table S1. Sequences of oligo DNAs and RNAs used in this study

Primers for plasmid construction

flamenco F: 5'-AATTCGCCAACGTTGTTGTT-3'
flamenco R: 5'-TGAAACAAAACGGAGAATGC-3'
Yb wt F: 5'-ATGGAGCCAATTGGAGATCT-3'
Yb wt R: 5'-CTACATATATGGACAGTCCT-3'
Dot CoM508 F: 5'- ATTCTCCTTTCTCAGGATGC-3'
Dot CoM508 R: 5'- GCATTGCTACCTTACGTTTC-3'
Dot CoM527 F: 5'- AAACGTTTGTTTATTTTCACGA-3'
Dot CoM527 R: 5'- TAAATTTAGAAGCACTGTGGATT-3'

qPCR primers

flamenco F: 5'-AAAGCGTCTGCTACATGATATAGTTT-3'
flamenco R: 5'-AGGTCCAGAAGGCATACGAC-3'
mdg1 F: 5'-AACAGAAACGCCAGCAACAGC-3'
mdg1 R: 5'-CGTTCCCATGTCCGTTGTGAT-3'
rp49 F: 5'-CCGCTTCAAGGGACAGTATCTG-3'
rp49 R: 5'-ATCTCGCCGCAGTAAACGC-3'

Primers for mutagenesis

Yb wt-r F:
5'-CCAAAGGCTATATAAATCAGGCGCTAATTCTCTGCGATGGCATGCTC-3'
Yb wt-r R:
5'-GAATTAGCGCCTGATTTATATAGCCTTTGGACCAGAGGAGCAGCAC-3'
Yb wt-mt F: 5'-ATAAGCTTATGGAGCCAATTGGAGATCTG-3'
Yb wt-mt R: 5'-ATGAATTCCTACATATATGGACAGTCCTTGG-3'
Yb Q399A-r F: 5'-GCCAGATTGCCTGGCCACATGTC-3'
Yb Q399A-r R: 5'-GACCGCCCGCGCTCGCG-3'
Yb P455A-r F: 5'-GCCAACCAGGGGCAGGGCAAA-3'
Yb P455A-r R: 5'-ACACACAAAGATGCAGGTAG-3'
Yb D537A-r F: 5'-GCCAACCTGAACGACATGGTTTCG-3'
Yb D537A-r R: 5'-CAAGGCTATGCACTTCACCG-3'

Probes for northern blotting

tj-piRNA: 5'-GGTAATGGGAATGCACTTCTCTTGAA-3'
mir310: 5'-AAAGGCCGGGAAGTGTGCAATA-3'
RpL5 F: 5'- ATGGGTTTCGTTAAGGTAGT -3'
RpL5 R: 5'- TTAAGCCTCAGTTTCAGACT -3'

Oligos for RNAi

siEGFP: 5'- GGCAAGCUGACCCUGAAGUTT-3'
5'- ACUUCAGGGUCAGCUUGCCTT-3'
siPiwi: 5'- GCUCCCAGGCGUGAAGGUGTT-3'
5'- CACCUUCACGCCUGGGAGCTT-3'
siYb: 5'- GGGGUACAUCAACCAAGCUTT-3'
5'- AGCUUGGUUGAUGUACCCCTT-3'
siZuc: 5'- UGAACUGGGCGAGAUCUGUTT-3'
5'- ACAGAUCUCGCCCAGUUCATT-3'
siflam1: 5'- CGUUGUUGUUUCAUGUUAGTT-3'
5'- CUAACAUGAAACAACAACGTT-3'
siflam2: 5'- CUCAAAAUUGGGUCCUUCATT-3'
5'- UGAAGGACCCAAUUUUGAGTT-3'
siflam3: 5'- CUUACGGUAAUAUCCGCAUTT-3'
5'- AUGCGGAUAUUACCGUAAGTT-3'
siflam4: 5'- CGGGUAUCUGAAAGUCGAUTT-3'
5'- AUCGACUUUCAGAUACCCGTT-3'
siflam5: 5'- CUCGACUAUAGCAUUCUCCTT-3'
5'- GGAGAAUGCUAUAGUCGAGTT-3'

Experimental Procedures

***Drosophila* strains**

Yellow white (*y w*) was used as a wild-type strain. The *flam* [KG00476] and the *fs(1)Yb*[72] alleles were kindly provided by A. Pelisson (Mevel-Ninio et al., 2007) and H. Lin (King et al., 2001), respectively. Fly stocks were maintained at 25 °C.

Cell culture and RNAi

OSCs were grown at 26° C in OSC medium prepared from Shields and Sang M3 Insect Medium (Sigma) supplemented with 0.6 mg/ml glutathione, 10%FBS, 10 mU/ml insulin and 10% fly extract. To perform RNAi in OSCs, trypsinized OSCs (3.0×10^6 cells) were suspended in 100 μ l of Solution V of the Cell Line Nucleofector Kit V (Amaya Biosystems) together with 200 pmol of siRNA duplex. The sequences of RNA oligos used for RNAi are shown in Supplementary Table S1. The transfected cells were transferred to fresh OSC medium and incubated at 26 °C. After 48 h, cells were re-transfected using the same amount of siRNA duplex and incubated at 26 °C for an additional 48 h.

Production of anti-Yb antibodies

Monoclonal antibodies against Yb were raised primarily as described previously (Ohtani et al., 2013). A recombinant protein consisting of GST and the N-terminal region of Yb (200 amino acids) was purified from *E. coli* and injected into mice.

RNA-FISH

The FITC- and DIG-labeled RNA probes were prepared using RNA labeling mixture (Roche) and SP6RNA polymerase (Roche) according to the manufacturer's instructions. To prepare a probe specific for the *flam* locus, OSC genomic DNA was used as a template for PCR. The primers used for PCR are indicated in Supplementary Table S1. *In situ* hybridization was carried out essentially as described previously (Sone et al., 2007), except that 3 µg/ml proteinase K and 100 µg/ml RNase A treatment were performed at 37 °C for 1 min and 30 min, respectively. RNase treatment was performed after hybridization. Blocking was performed with 1% Blocking Reagent (Roche) at room temperature. Anti-FITC polyclonal antibody (Abcam ab19491) (1:500 dilution) and anti-DIG monoclonal antibody (Abcam ab420) (1:500 dilution) were used as primary antibodies. Alexa Fluor488-conjugated anti-rabbit IgG (Molecular Probes) (1:200 dilution) and Cy3-conjugated anti-mouse IgG (SIGMA) (1:200 dilution) were used as secondary antibodies. Samples were mounted with SlowFade® Gold antifade reagent with DAPI (Invitrogen). All images were collected using a Zeiss LSM 710 laser microscope.

DNA-FISH

Digoxigenin- or biotin-labeled DNA probes were prepared using Nick Translation Mix (Roche) according to the manufacturer's instructions. To prepare the probes, BAC clones DME1-021J16 (upstream of the *flam* locus) and DME1-014M21 (downstream of

the *flam* locus), were used as templates. BAC clones were obtained from the National BioResource Project (NBRP) *Drosophila*, Japan. OSCs were treated with ice-cold 0.75 M KCl for 5 min and then, after resuspending in acetic acid-methanol (1:3), spread onto slides. The slides were treated according to the procedures of Masumoto *et al.* (Masumoto *et al.*, 1989), except that denaturing was performed at 73 °C for 3 min. Washing was performed twice using 50% formamide-containing 2x SSC at 37 °C for 7 min, which was followed by a wash with 2x SSC at 37 °C for 7 min. After washing, the hybridized probes were detected by immunofluorescence analysis. The samples were blocked with 5% dried skimmed milk in 4x SSC at room temperature for 1 h. Anti-digoxigenin antibody (Abcam ab420) (1:1,000 dilution) was used as a primary antibody. Alexa Fluor488-conjugated anti-mouse IgG (Molecular Probes), streptavidin-Cy3 (Jackson ImmunoResearch) and Cy3-conjugated anti-mouse antibodies were used as secondary antibodies (1:200 dilution).

Immunofluorescence

Immunofluorescence on OSCs and ovaries was performed primarily as described previously (Ohtani *et al.*, 2013; Saito *et al.*, 2009) using an anti-Yb antibody raised in this study. Alexa Fluor546-conjugated anti-mouse IgG (Molecular Probes) was used as a secondary antibody. The cells were mounted with SlowFade® Gold antifade reagent with DAPI. All images were collected using a Zeiss LSM 700 laser scanning microscope.

Body Counting

Confocal images of immunofluorescence were transferred to the Columbus System (PerkinElmer Japan) and analyzed by Building Block (PerkinElmer Japan). Nuclei were masked and then perinuclear signals for Yb bodies and Flam bodies were detected.

Electron microscopy *in situ* hybridization

For transmission electron microscopy (TEM) analysis, OSCs cultured in a slide chamber were used. OSCs were fixed with 4 % paraformaldehyde (PFA) in 0.1 M phosphate-buffered saline (PBS) pH 7.4 overnight, and then washed with RNase-free PBS. The samples were hybridized with FITC-conjugated specific RNA probe as described above, except that 0.5 % Triton-100 was used for 5 min. Samples were incubated for 24 hours at 4 °C with a primary rabbit anti-FITC (1:500) antibody and then washed 12 times in 0.1 M phosphate buffer (PB) containing 0.005% saponin for a total of 2 hours. Samples were incubated for 24 hours at 4 °C with nanogold-conjugated anti-rabbit secondary antibody (1:100, Invitrogen). After washing in PB, cells were fixed with 2.5% glutaraldehyde for 10 minutes at 4 °C, followed by a 10 min incubation in the dark with the HQ-Silver kit (Nanoprobes Inc.). After 90 min of additional fixation with 1.0% osmium tetroxide, the cells were sequentially dehydrated in ethanol, acetone, and QY1, and then embedded in Epon. Ultrathin sections of OSCs were prepared at a thickness of 70 nm and stained with uranyl acetate, lead citrate and tannin acid for 10, 10 and 4 minutes, respectively. The sections were observed under a transmission electron microscope (JEOL models 1230 and 1400 Plus), and the images were

captured using Digital Micrograph 3.3 (Gatan Inc.).

Immuno-electron microscopy

OSCs were fixed with 0.1% glutaraldehyde and 4% PFA in 0.1 M PBS (pH 7.4) for 20 minutes, followed by incubation with 5% Block Ace containing 0.1% saponin in 0.1 M PB for one hour. The cells were stained with primary mouse anti-Yb antibody (1:250) for 24 hours and nanogold conjugated anti-mouse secondary antibody (1:100, Invitrogen) for 24 hours at 4 °C. After fixation in 2.5% glutaraldehyde, nanogold particles were enhanced using the HQ-Silver kit for 10 minutes, post-fixed with 1.0 % osmium tetroxide, dehydrated through an ethanol series, and embedded in Epon. The procedures for preparation of the ultrathin sections and their observation are described above in “Electron microscopy *in situ* hybridization”.

Western blot analysis

Western blotting was performed primarily as described previously (Miyoshi et al., 2005). Anti-Piwi (Saito et al., 2006) and anti-Yb (this study) anti-bodies were used as a primary antibody. Anti-tubulin was obtained from the Developmental Studies Hybridoma Bank and used at 1:2,000 dilution.

Northern blot analysis

For *flam* transcript detection, total RNAs from OSCs before and after RNAi treatment were isolated using ISOGEN (Nippon Gene). rRNAs were removed from total RNAs

using the Ribo-Zero rRNA Magnetic Kit (Human/Mouse/Rat) (AR BROWN). RNAs were separated on 1% agarose gels and transferred using the iBlot Dry Blotting System (Invitrogen). After UV crosslinking, hybridization was performed at 65 °C in 500 mM Church phosphate buffer, 1 mM EDTA (pH 8.0) and 7% SDS with random-labeled antisense oligodeoxynucleotide probe, and washed at 65 °C in 2x SSC containing 0.1 % SDS and in 0.1x SSC containing 0.1% SDS. Probes were labeled using the Random Primer DNA Labeling Kit Ver.2 (TaKaRa). The blots were exposed on BAS-MS2040 imaging plates and signals were quantified using a BAS-2500 system (Fuji). For detection of small RNAs, total RNAs from OSCs were isolated using ISOGEN and northern blot analysis was performed using 5 µg of total RNAs as described previously (Saito et al., 2009).

Plasmid construction

An expression vector for myc-Yb wt was generated by inserting the wild-type Yb coding region into the pAcM vector (Saito et al., 2009). myc-Yb-r was constructed as essentially described previously (Saito et al., 2010). Briefly, 5' and 3' fragments of *Yb* cDNA were individually amplified by KOD plus DNA polymerase (Toyobo) using the following primers: Yb-F and Yb-mt-R for the 5' fragment, and Yb-mt-F and Yb-R for the 3' fragment. The resulting DNA fragments were mixed and used as templates for PCR amplification with Yb-F and Yb-R. The amplified fragment (siRNA-resistant *Yb* cDNA) was cloned into the HindIII-EcoRI-digested pAcM vector. The point mutation was introduced into the siRNA-resistant *Yb* cDNA using a KOD-Plus-Mutagenesis Kit

(Toyobo). Primers are listed in Supplementary Table S1.

qRT-PCR analysis

Total RNAs from OSCs were isolated using ISOGEN. Total RNAs were then treated with DNase to eliminate DNA contamination. Reverse transcription of total RNAs (500 ng) was performed using a PrimerScript RT Master Mix (TaKaRa). The resulting cDNAs were amplified using a LightCycler 480 Real-Time PCR Instrument II (Roche) with SYBR Premix Ex Taq (TaKaRa). The primers used are listed in Supplementary Table S1. The experiments were carried out at least three times.

CLIP

CLIP was performed primarily as described previously (Jaskiewicz et al., 2012). Anti-Yb was used to immunopurify Yb from OSCs after irradiation by UV (254 nm) for crosslinking. In the experiment shown in Figure 4B, Yb wt-r, Yb Q399A-r, Yb P455A-r and Yb D537A-r were expressed by transfection into Yb-depleted OSCs. RNAs within the immunoprecipitates were labeled with ^{32}P as described (Jaskiewicz et al., 2012), and the signal intensity was quantified using a BAS-2500 system (FUJIFILM).

Bioinformatic analysis

The Yb-CLIP library was sequenced using the Illumina HiSeq2000 platform according to the manufacturer's instructions. The average base-wise quality was checked, and those that passed quality control were subjected to the following analysis. Raw Yb-CLIP tags

were processed using the NCBI BLAST program to detect fragments of adaptor sequences, and the detected sequences were removed. Reads were then mapped to the Release 5 assembly of the *Drosophila melanogaster* genome (excluding chuUextra) and to GenBank entry L03284 (the only GenBank entry that recovers hits not present in Release 5), using Burrows-Wheeler Aligner (BWA) software (Li and Durbin, 2009). Up to two mismatches were allowed. Read realignment was performed using The Genome Analysis Toolkit (McKenna et al., 2010). To remove potential duplicates resulting from PCR amplification, we collapsed identical reads and mappable reads with the same starting genomic positions. The annotation of Yb-CLIP tags was determined as previously described (Saito et al., 2009). Briefly, the overlap between mapped regions of the reads was examined using reference data obtained from the UCSC Genome Browser (Meyer et al., 2013) and Ensembl databases (Flicek et al., 2013). Reads were assigned to a feature when the length of its overlap was longer than 90% of the tags. To detect overlap between Piwi-piRNA reads and Yb-CLIP tags, we made use of previously published mapping data (Saito et al., 2009). Piwi-piRNA reads and Yb-CLIP tags, which were mapped to a single genomic locus, are shown for the *flam* cluster region (chrX: 21,505,666-21,684,449) and surroundings. Number of Yb-CLIP tags mapped to each piRNA clusters (Malone et al., 2009), and geneic piRNA producing transcripts (Robine et al, 2009) are counted.

Supplemental References

Flicek, P., Ahmed, I., Amode, M.R., Barrell, D., Beal, K., Brent, S., Carvalho-Silva, D., Clapham, P., Coates, G., Fairley, S., et al. (2013). Ensembl 2013. *Nucleic Acids Res.*

41, D48–55.

King, F.J., Szakmary, A., Cox, D.N., and Lin, H. (2001). Yb modulates the divisions of both germline and somatic stem cells through piwi- and hh-mediated mechanisms in the *Drosophila* ovary. *Mol Cell*. 7, 497-508.

Li, H., and Durbin, R. (2009). Fast and accurate short read alignment with Burrows-Wheeler transform. *Bioinformatics* 25,1754-1760.

McKenna, A., Hanna, M., Banks, E., Sivachenko, A., Cibulskis, K., Kernytsky, A., Garimella, K., Altshuler, D., Gabriel, S., Daly, M., et al. (2010). The Genome Analysis Toolkit: a MapReduce framework for analyzing next-generation DNA sequencing data. *Genome Res*. 20,1297-1303.

Meyer, L.R., Zweig, A.S., Hinrichs, A.S., Karolchik, D., Kuhn, R.M., Wong, M., Sloan, C.A., Rosenbloom, K.R., Roe, G., Rhead, B., et al. (2013). The UCSC Genome Browser database: extensions and updates 2013. *Nucleic Acids Res*. 41, D64–69.

Saito, K., Nishida, K.M., Mori, T., Kawamura, Y., Miyoshi, K., Nagami, T., Siomi, H., and Siomi, M.C. (2006). Specific association of Piwi with rasiRNAs derived from retrotransposon and heterochromatic regions in *Drosophila* genome. *Genes Dev*. 20, 2214-2222.